NTNU – Trondheim
Norwegian University of
Science and Technology

Numerical studies of Supernova Remnants

Haakon Andresen

Physics
Submission date: May 2013
Supervisor: Michael Kachelriess, IFY

Norwegian University of Science and Technology
Department of Physics

Abstract

Supernovae are very luminous events, on the scale of entire galaxies, and deposit mass and large amounts of energy in to the surrounding interstellar medium. In this work the effect of a supernova on the surrounding medium is studied. The evolution of the remnant is assumed to be spherical symmetric. The hydrodynamic evolution of the system is simulated for different density distributions of the ambient medium and compared to analytically solutions where they exists.

Some background theory about stellar evolution and supernovae is given. Since strong shocks from supernovae is interesting in the context of cosmic ray acceleration some theory about cosmic is included.

The framework for simulating the hydrodynamic equations governing the system is based on the work done by W.Benz [2].

Sammendrag

Supernovaeksplosjoner er lyssterke hendelser der en enkelt stjerne, over en relativt liten tidsperiode, kan bli like lyssterk som en hel galakse. Slike eksplosjoner sender store mengder masse og energi ut i det interstellare medium. I denne oppgaven blir det studert hvordan en supernova påvirker omgivelsene, oppgaven begrenser seg til kule-symmetriske supernova levninger. Det blir utført simuleringer for forskjellige strukturer av mediet rundt supernovaen og det sammenlignes med analytiske løsninger, der de eksisterer. Metoden for å simulere utviklingen av systemet baserer seg på rammeverket som W.Benz presenterer i [2]. Denne metoden blir gjennomgått i detalj.

Noe bakgrunnsteori om stjerners utvikling og supernovaeksplosjoner blir gitt og siden sjokkbølger fra supernova eksplosjoner er interessant i henhold til kosmisk stråling blir det også gitt teori om kosmisk stråling.

Acknowledgments

First and foremost I would like thank my supervisor Professor Michael Kachelrie for his patient supervision. His help has been invaluable not only when working with my thesis, but also in taking the next academic step.

I am also grateful to NTNU, especially the department of theoretical physics, for giving me an interesting and solid education in physics. I have truly enjoyed my five years in Trondheim and made many good friends, in particular the guys of study room B3-131.

My family should also be mentioned, they have always been supportive and interested in my education.

Contents

List of Figures

Introduction

A supernova is an event where a star undergo drastic changes and over a short period of time the luminosity of the star can become comparable to an entire galaxy. The supernova progenitors are thought to be either white dwarfs or massive stars at the end of their life, this separates supernovae events into two classes.

A white dwarf is supported by degenerated electron pressure, however there is a upper limit on how much mass can be supported this way and if this limit is surpassed the dwarf will start to collapse. The collapse enables carbon fusion and the released energy is enough to overcome the gravitational binding energy, destroying the star. This produces a very characteristic light curve and as such type Ia supernovae, as they are called, are good standard candles. When massive stars exhaust the hydrogen in their core nuclear process will slow down and the core will collapse under its own gravitational pull. During this collapse a large amount of gravitational energy is released, this type of supernova is a core collapse supernova. Common for both types is the fact that they eject matter into the interstellar medium and create a shock wave. How a supernova effect its soundings is important for the evolution of galaxies and star formation. The prorogation of strong shock is also interesting with respect to acceleration of cosmic rays.

We start this thesis with some background theory and move on to the numerical simulation of the hydrodynamic equations governing the evolution of a supernova remnant. The numerical simulation of fluids is in itself an interesting topic and has applications to several fields in physics.

Chapter 1

Stellar evolution

The evolution of stars can be divided into three parts: Formation, main sequence phase and post main stage. Particularly interesting with respect to supernovae are the death of high mass stars, white dwarfs and the role supernova feedback plays on star formation.

1.1 Main sequence

The term *main sequence comes* from observations: It is possible to infer the luminosity and the temperature of the star from the light we observe. The first is found by realizing that the light emitted from a star at a given distance from earth will be spread out over the surface of a sphere with radius r, if r is the distance to the star. As such the incoming flux should be related to the luminosity as follows:

$$L = 4\pi r^2 \mathcal{F}, \tag{1.1}$$

here $\mathcal{F}$ denotes the observed flux and L is the luminosity of the star.

The temperature is found by the fact that a star is very close to a black body, an object that absorbs all radiation it receives. Therefore we can approximate its spectrum as the one of a black body at a given temperature and get a good estimate of the surface temperature of the star. In 1900 Max Planck developed an empirical formula to describe black body spectra:

$$I(\lambda, T) = \frac{2hc^2}{\lambda^5 \left(e^{hc/\lambda k_B T} - 1\right)}, \tag{1.2}$$

where λ is the wave length of the emitted light, h is Planck's constant, T is the temperature of the object and c is the speed of light. For a given wavelength λ_m, equation (1.2) has a

maximum. This wavelength fulfills the following equation:

$$\lambda_m T = \text{constant}, \tag{1.3}$$

this is known as Wien's displacements law. By looking at the spectrum of a star and finding the wavelength at which it emits most light we can estimate the temperature.

A diagram plotting the luminosity as a function of temperature is known as Hertzsprung-Russell-diagram or HR-diagram for short, named after the two astronomers that first proposed it, see figure 1.1.

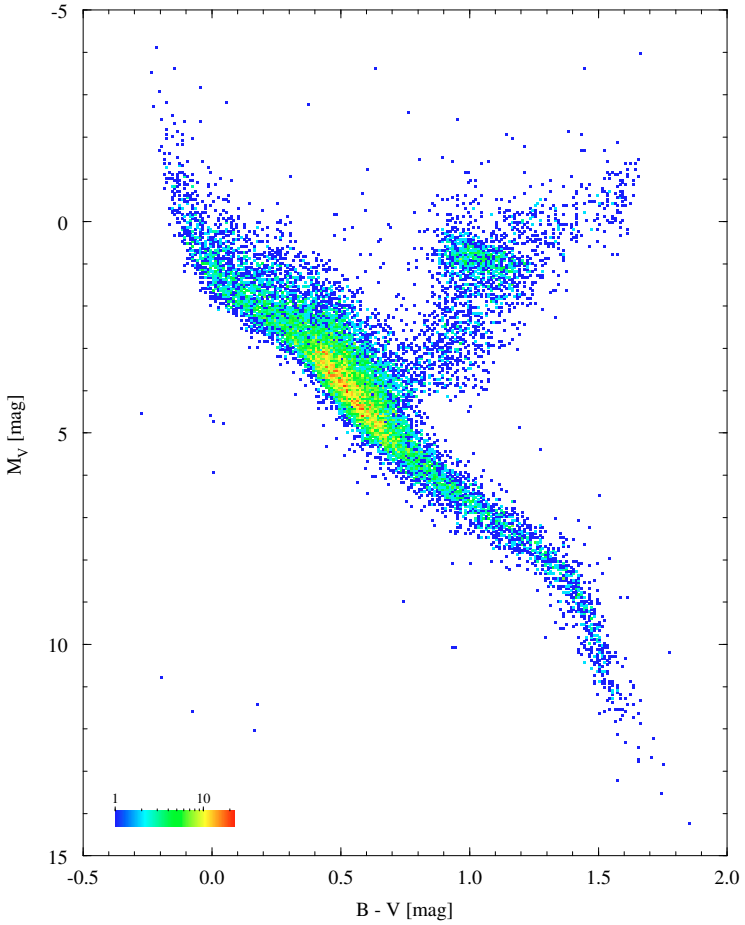

Figure 1.1: HR diagram for 41704 stars, from the Hipparcos Catalogue [7]

The stripe in figure 1.1 is called the main sequence and this is where the term main sequence star comes from. When a star is on the main sequence its energy source is hydrogen burning in the core and it will stay on the main sequence as long as it has hydrogen to burn. To find out how long a star will stay on the main sequence we need to know how much fuel is available and the rate that fuel is being burned. Based on observations it is

possible to infer a relation between the luminosity and the mass of a star,

$$L/L_\odot = \left(\frac{M}{M_\odot}\right)^\alpha, \tag{1.4}$$

where $L_\odot$ and $M_\odot$ denotes the luminosity and mass of the sun. The parameter α is found to have different values:

$$\alpha = \begin{cases} 1.8, & \text{if } M < 0.3M_\odot \\ 4.0, & \text{if } 0.3M_\odot < M < 3M_\odot \\ 2.8, & \text{if } M > 3M_\odot, \end{cases} \tag{1.5}$$

see [11]. In other words, the more massive stars radiate away more energy and burn the hydrogen in the core faster than less massive stars. Even though more massive stars have more hydrogen available to burn, the results is that less massive stars have a longer lifespans than more massive stars. A conclusion supported by investigating stellar populations in young and old galaxies.

1.2 Star formation

Consider a uniform and spherical gas cloud, let M denote the mass of the cloud. We are interested in determining the stability of such a cloud, if the cloud is unstable it can collapse and cause star formation. If electromagnetic forces can be neglected, the validity of this assumption is questionable and will be discussed below, then the only effect resisting gravitational collapse is the random thermal motion within the cloud.

Gravitational binding energy is equal to the energy required to bring the mass in from infinity to the final configuration. In spherical coordinates the mass of a spherical volume containing a uniform gas is given by:

$$M = \frac{4\pi}{3} r^3 \rho \Rightarrow dM = 4\pi r^2 \rho dr,$$

where ρ is the density of the gas.

Remembering that the gravitational energy between two point masses, m_1 and m_2, is given by:

$$U = -G\frac{m_1 m_2}{r}, \tag{1.6}$$

where G is the gravitational constant. Now we take m_1 to be the mass already assembled and m_2 to be the mass being the mass of a shell being brought in. Since the end result should not depend on how the final state was assembled we can imagine that we assemble the inner part first, then adding on spherical shells of thickness dr. As such

$$dU = -G4\pi\frac{4\pi}{3}\rho^2 r^4 dr, \tag{1.7}$$

and we get the following expression for U:

$$U = -\int_0^R dU = -\int_0^R G4\pi\frac{4\pi}{3}\rho^2 r^4 dr = -\frac{3}{5}\frac{GM^2}{R},$$

where R denotes the radius of the sphere.

1.2.1 Jeans length

For the cloud to be gravitational bound the total thermal energy,

$$E_t = \frac{3}{2}\frac{M}{m}k_B T, \tag{1.8}$$

has to be less than the gravitational binding energy.

$$\frac{3}{5}\frac{GM^2}{R} > \frac{3}{2}\frac{M}{m}k_B T. \tag{1.9}$$

The limit between stable and unstable is found by equating the left and right hand side of equation (1.9), then solving for R we find a limit between bound and unbound. This radius is known as the Jeans radius and is given by:

$$R_j = \left[\frac{15k_b T}{8\pi G m\rho}\right]^{\frac{1}{2}}. \tag{1.10}$$

Magnetic energy density is given by

$$u_B = \frac{B^2}{2\mu_0}, \tag{1.11}$$

where B is the magnetic field and μ_0 is the magnetic vacuum permeability. We expect the magnetic effects to become important if the energy from magnetic fields in the cloud are on the same order as the gravitational binding energy.

The total magnetic energy of a cloud is given by

$$U_b = u_b V = \frac{2\pi B^2 R^3}{3\mu_0}. \tag{1.12}$$

Equating equation (1.12) and (1.8) and solving for B yields

$$B = \left[\frac{9}{10}\frac{GM\mu_0}{\pi R^4}\right]^{\frac{1}{2}}. \tag{1.13}$$

For a cloud with radius $R = 10$ pc and consisting of molecular hydrogen, with a density of around 300 particles per cubic centimeter, we get

$$B \approx 6 \times 10^{-5}\mathrm{G}.$$

This is of the same order as observed magnetic fields, see [11]. As such the effect of magnetic fields should be taken into consideration.

1.2.2 Fragmentation and star formation

Next consider a region, part of a larger cloud, that is subject to a perturbation and as a result the density in the region increases. An example of a perturbation could be a shock wave from a nearby supernova explosion. As a result of compression the perturbed region can exceed its Jeans limit and start to collapse. Some regions within the can cloud start to collapse while others remain stable, creating regions of high and low densities. The gravitational pull of the dense areas increases and they attract more mass leading to fragmentation of the cloud. These fragmentation can continue to accrete mass and grow, in the process both temperature and density increases, until the core temperature reaches the threshold for hydrogen ignition and a main sequence star is born.

M. R. Bate et al. has preformed simulations of such fragmentation, modeling the fragmentation of a $50M_{\odot}$ mass cloud with diameter 0.375 pc. See [1]. Numerical results are shown in figure 1.2.

1.3 Stellar death

When a star depletes the available hydrogen in its core, nuclear processes slow down and the core starts to contract. For low mass stars the contraction is gradual and slow, but for more massive stars the process is faster and this gives rise to an important distinction between high and low mass stars: In low mass stars the core has time to reach a degenerated state before helium burning starts. For high mass stars this is not the case, helium burning temperatures are reached before the core become degenerated.

Degeneracy is a quantum mechanical effect that occurs at high density. Pauli's exclusion principle states that two fermions can not be in the same state, electrons are fermions. This effect causes the average energy of the electrons to be much greater than what one would expect from the temperature. Higher energy means higher momentum and therefor higher pressure. The degenerated electron pressure is given by:

$$P = \frac{h^2}{20m_e}\left[\frac{9\rho^5}{\pi^2 m_H^5 \mu_e^5}\right]^{\frac{1}{3}}, \tag{1.14}$$

where m_H is the atomic mass, m_e the electron mass, ρ the density, and μ_e^{-1} is the average number of free electrons per nucleon, see [13].

High mass stars contract rapidly, pressure and temperature increase to the point where helium burning starts. The burning of helium heats the layers around the core to a temperature where hydrogen burning can take place. The pressure from burning of helium stabilizes the core, however the core will quickly deplete its helium fuel. The core contracts further and the temperature rise to the point where carbon and oxygen burning can start. The layer burning hydrogen is heated further and helium burning starts. This process of burning and depleting heavier and heavier elements in the core continues, developing a

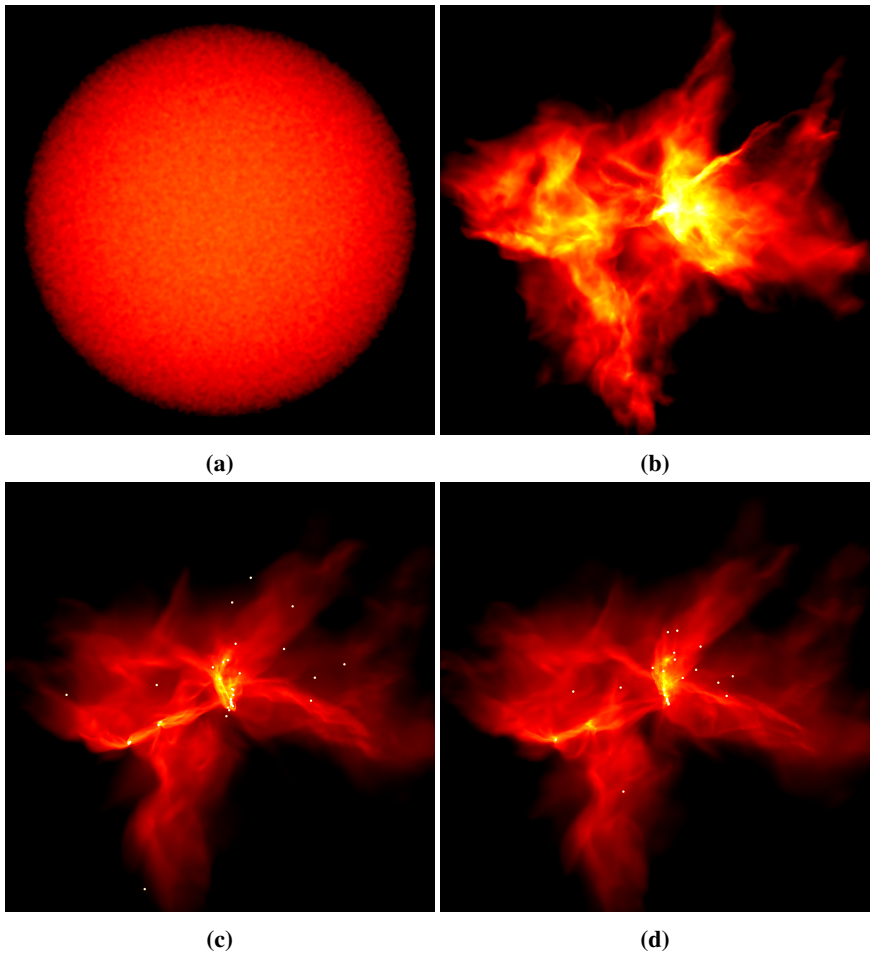

Figure 1.2: Cloud collapse simulation, taken from [1] with permission. (a) Initial cloud. (b) Collapse has stared. (c) Bright regions indicate star formation. (d) Increasing amount of star formations.

shell structure with a degenerated iron core surrounded by shells burning lighter elements. Nuclear burning in the outer shells keeps the core growing until degeneracy pressure can no longer balance out the gravitational pull. At this point the iron core has a typical diameter of 3000 km and a density of the order $10^9 \mathrm{g/cm}^3$.

The shell burning can release more energy than the core did during the main sequence phase and as a result the outlaying layers of the star heat up. This causes the star to expand, which in turn cools the gas. The star increases in size and becomes a red giant. The outer layers are loosely bound to the rest of the star and the momentum transfer from photons, from the interior of the star, can cause the outer layers to be ejected. The fate of the star is determined by its mass, the core will eventually start to collapse. For very massive stars gravitational collapse can not be halted and the end result is a black hole. For a less massive star the gravitational collapse can eventually be stopped and we are left

with a neutron star.

Low mass stars contracts slower, therefore the core is in a degenerated state when helium burning start. Since the pressure in a degenerated gas is not depended on the temperature the pressure do not increase and there is nothing slowing the reaction rate. The result is that the helium-carbon process takes place over a very small time period, this is known as a helium flash. After the burst the core is no longer degenerated, the remaining helium is steadily converted into oxygen and carbon. Eventually the helium full is depleted, at this point the temperature is not high enough for further fusion and the core starts to collapse once more.

The collapse is eventually halted by degenerate the electron pressure and we are left with a compact object, known as a white dwarf. Subrahmanyan Chandrasekhar derived a limit on how much mass can be supported by degenerate electron pressure, found to be around $1.44M_{\odot}$.

Chapter 2

Supernovae

A supernova is an very luminous event, during which the luminosity of a star can become comparable to luminosity levels of an entier galaxy. The event takes place over a short time and it is clear that during supernova explosion the progenitor star undergo drastic changes. The study of supernovae events are important in several branches of astrophysics. The abundance of the elements in the universe is one example, elements heavier than iron can not be produced in normal stars. In astronomy type Ia are useful as standard candles and were important for discovering that the expansion of the universe is accelerating.

Classification of such events are based on the observed properties, such as light curves and spectral lines, with two main classes: type I and II. Historically supernovae were labeled type I if there were no hydrogen lines and type II if hydrogen lines were observed. Further observations showed different types of spectra within these two main classes, figure 2.1 shows spectra for type Ia, Ib and II supernovae.

A detailed classification of supernovae, based on observational properties, is given by [5].

2.1 Detonation mechanism

Another way to classify supernovae is by the detonation mechanism, resulting in two classes: Core collapse and thermonuclear detonation. The reason for the large amount of observational classes, relative to detonation mechanisms, is that a dying star might be subject to effects like stellar wind. The surrounding medium can therefore be different from case to case. Strong stellar wind can blow away the hydrogen rich outer layer of, explaining the lack of hydrogen lines in type II.

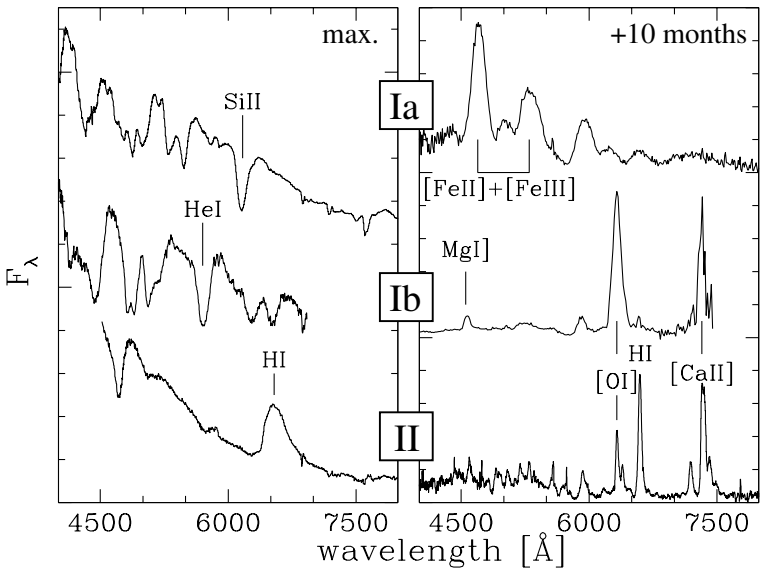

Figure 2.1: Supernovae spectra for type Ia, Ib and II. Figure by E. Cappellaro and M. Turatto [5].

White dwarfs and thermonuclear detonation. Progenitors to type Ia supernovae are thought to be white dwarfs accumulating mass, until exceeding the Chandrasekhar limit. When this happens the electron degeneracy pressure can no longer support the star against its own gravitational pull and it starts to collapse. The temperature rises and nuclear burning of carbon starts up. This rises the temperature further, the increased temperature speeds up the nuclear process. The increase in temperature will not affect the pressure and as such the process continues unhindered and turns into a runaway situation. The nuclear processes occurring throughout the star releases a large amount of energy, $E \approx 10^{44}$ J [13]. The released energy is greater than the binding energy of the dwarf and the star is blown apart.

While it is generally agreed upon that a type Ia supernova is produced by a white dwarf accumulating mass, it is still not fully understood how the dwarf accumulates the mass. Early models proposed a binary system including a white dwarf, where the dwarf accretes mass from the companion. However such models had problems raising the mass of the white dwarf sufficiently. Several models to solve the problem have been proposed, a review of various progenitor models can be found in [16].

Core collapse. As a massive star nears the end of its life it will develop an iron core supported by electron degeneracy pressure. This core will continue to grow until the degenerate pressure can no longer support the it.

When the core starts to collapse the temperature increases, enabling photo disintegration of iron nuclei. This process consumes energy and reduces the particle number, as such

the pressure drops and the collapse speeds up. The density continues to increases, finally when the density is $\rho \sim 10^{14}\mathrm{g/cm}^3$ the collapse is halted. The core collides with the outer layers that are still falling in and a shock is created. This shock travels outwards trough the layers surrounding the core, however it is rapidly losing energy by destroying iron nuclei. At around 100 km the shock stagnates and creates a boundary where the outer layers accretes on the inner core.

In order for the core to turn into a supernova some of the gravitational energy released in the collapse has to be deposited into the shock. To estimate the energy released in such an event we subtract the energy absorbed by nuclear processes, such as photo disintegration, from the released gravitational energy. Remembering the gravitational potential energy of a sphere, with mass M and radius R,

$$E_g = -\frac{3}{5}\frac{GM^2}{R}. \tag{2.1}$$

It is clear that a contracting sphere will release gravitational energy, for a typical iron core collapsing into a neutron star $\Delta E_g \approx 10^{46} J$. While the absorbed nuclear energy is of the order $E_n \approx 10^{45}$ J, see [13]. A portion of this energy is carried away by neutrinos and deposited behind the shock front. Simulations have shown that this effect can accelerate the shock and results in a successful detonation. For a more detailed discussion see [8].

The energy released in such an event is more than enough to eject the envelope surrounding the core. Observations suggest that material is being ejected with velocities up to 10 000 km/s.

Chapter 3

Cosmic rays

In 1909 Theodor Wulf famously measured higher levels of radiation on top of the Eiffel tower than at ground level. While the source and validity of this deviation were debated at the time, it was the first historical observation of radiation not coming from Earth. This radiation later became know as cosmic rays. Cosmic rays interact strongly with the atmosphere, and observations have therefore historically taken place at high altitudes. In 1912 Victor Hess measured that radiation increased with altitude, furthermore he noted that the intensity did not decrease during a solar eclipse or night time, ruling out the sun as the source. Modern experiments have given us a good overview of the composition of cosmic rays. Around 79 % of charged cosmic rays consists of free protons and helium account for about 70 % of the remaining rays. A small amount of the charged cosmic rays are electrons and positrons, see [10]. Figure 3.1 shows the observed intensity for hydrogen, helium, carbon and iron cosmic rays. We see a significant higher intensity of cosmic rays consisting of hydrogen and helium. We also see that for energies above 10 GeV the spectrum fits a power law, with a deviation at lower energies. This is due to the sun, solar wind interacts with cosmic rays and decelerates them. For high energy particles this effect is not as significant as for low energy particles. The

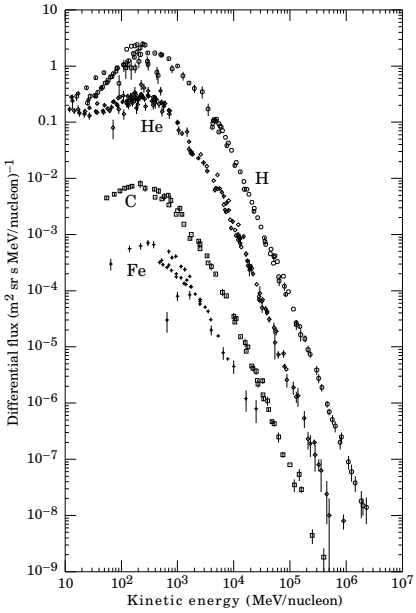

Figure 3.1: Cosmic ray intensity. From [10]

result is that the sun partly screens the solar system from low energy cosmic rays. Due to the change in solar activity this effect is time depended and as such the observed spectra at low energies will be time depended and strongly anti-correlated with solar activity.

3.1 Acceleration of cosmic rays

In 1949 Fermi calculated the energy gain for particles interacting with magnetic clouds in the interstellar medium. He showed that the average energy per interactions, for relativistic particles interacting with a magnetic cloud with velocity V, is given by:

$$\left\langle \frac{\Delta E}{E} \right\rangle = \frac{8}{3} \left(\frac{V}{c} \right)^2, \tag{3.1}$$

where c is the speed of light.

Fermi assumed that such collision were the main source of energy gain, however several problems exists with this idea. The energy gain would be slow, due to the long mean free path of cosmic rays and low velocity of galactic magnetic clouds. It was also problematic to explain the energy spectrum of cosmic rays. See [12] for a more detailed discussion.

Shock acceleration of cosmic rays is interesting in the context of supernova remnants. Consider a strong shock propagating through a diffuse medium at sub-relativistic speeds, with high energy particles on both sides of the shock wave. High energy particles will not notice the shock front, because the shock front is very thin. Once they cross the front it is assumed that scattering effects, like streaming instabilities and turbulent motion, scatters the particles sufficiently so that their velocity distributions become isotropic in the frame of the moving fluid behind the shock. If the shock is moving trough the fluid with velocity V, we know that the fluid behind the shock travels with $V_2 = \frac{3}{4}V$. See chapter 4.

Let E_1 and E_2 denote the initial and finally energy in the lab frame, likewise E_1' and E_2' denotes the initial and final energy in the rest frame of the fluid behind the shock front. If a particle crosses the shock with an angle ϕ, scatters and exits with an angle β, see figure 3.2, then the Lorentz transformations are given by:

$$E_1' = \gamma(E_1 + V_2 E_1/c \cos\phi) \tag{3.2}$$
$$E_2 = \gamma(E_2' - V_2 E_2'/c \cos\beta). \tag{3.3}$$

For non relativistic motion $\gamma \approx 1$ and elastic scattering implies that $E_1' = E_2'$.

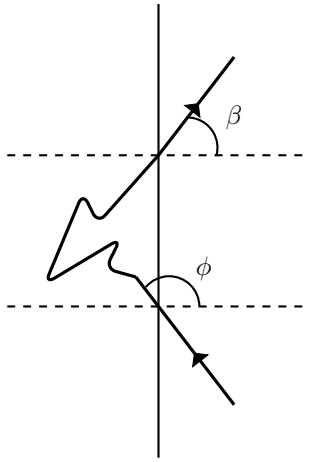

Figure 3.2: First order Fermi acceleration on shock front

Now we want to find the energy change,

$$\begin{aligned}\Delta E = E_2 - E_1 &= (E_2' + E_2'/cV_2\cos\phi) - E_1 \\ &= \frac{E_1 V_1}{c}(\cos\phi - \cos\beta).\end{aligned} \tag{3.4}$$

As such we get,

$$\frac{\Delta E}{E_1} = \frac{V_1}{c}(\cos\phi - \cos\beta). \tag{3.5}$$

Taking the average over all possible angles and remembering that the collision rate is proportional to $[1 - V/c\cos\phi]$ yields

$$\left\langle \frac{\Delta E}{E_1} \right\rangle = \frac{4}{3}\frac{V_1}{c}. \tag{3.6}$$

This expression is only first order in V_1/c and therefore a strong shock is a more effective source for particle acceleration. Strong shocks in supernova remnants have for a long time been good candidates as sources for galactic cosmic rays and recently direct observational evidence has been found [9].

Chapter 4

Fluid mechanics

If we have a system of N particles, we can in principle describe it by the motion of all the individual particles. However, for a large number of particles, it is easier to examine the macroscopic behavior of the system. By averaging over the motion of particles we can define quantities like pressure and temperature. Instead of modeling the movement of individual particles, we look at the flow of fluid elements. Each fluid element should contain a large number of particles, so that averaging is meaningful. However it should be small enough, so that relevant quantities do not change significantly within the element.

4.1 Eulerian and Lagrangian formulation of fluid mechanics

There are two common ways to formulate fluid mechanics: Eulerian and Lagrangian. The Eulerian formulation looks at a volume element fixed in space and describes how different variables change with time. In other words: One looks at the properties of small volumes at specific coordinates. The Lagrangian formulation picks a fluid element and follows it, looking at how variables changes for this element. The coordinate system moves with the element.

The two formulations are connected by the derivatives: If $\frac{\partial}{\partial t}$ denotes the time derivative in the Eulerian formulation and $\frac{D}{Dt}$ denotes the time derivative in the Lagrangian formulation we have the following connection

$$\frac{D}{Dt} = \frac{\partial}{\partial t} + \mathbf{v} \cdot \nabla. \tag{4.1}$$

To see this we start with the definition of the derivative action on a a scalar function: $\frac{D}{Dt}$ $f(\mathbf{r},t)$ where $\mathbf{r}=\mathbf{r}(t)$. Note that we have chosen to look at a scalar function, but it can be done in the same way for a vector.

$$\frac{Df(r,t)}{Dt}=\lim_{\Delta t\to 0}\frac{f(\mathbf{r}+\Delta\mathbf{r},t+\Delta t)-f(\mathbf{r},t)}{\Delta t}. \tag{4.2}$$

Now we use the fact that $\Delta\mathbf{r}=\mathbf{v}\Delta t$ and Taylor expand to first order. We get

$$\begin{aligned}\frac{Df(r,t)}{Dt} &= \lim_{\Delta t\to 0}\frac{f(\mathbf{r},t)+\Delta t\frac{\partial}{\partial t}f(\mathbf{r},t)+\Delta t\mathbf{v}\cdot\nabla f(\mathbf{r},t)-f(\mathbf{r},t)}{\Delta t}\\ &= \lim_{\Delta t\to 0}\frac{(\frac{\partial}{\partial t}f(\mathbf{r},t)+\mathbf{v}\cdot\nabla f(\mathbf{r},t))\cdot\Delta t}{\Delta t}\\ &= \frac{\partial}{\partial t}f(\mathbf{r},t)+\mathbf{v}\cdot\nabla f(\mathbf{r},t).\end{aligned}$$

Thus we arrive at the connection between the Eulerian and Lagrangian formulations:

$$\boxed{\frac{Df(r,t)}{Dt}=\frac{\partial}{\partial t}f(\mathbf{r},t)+\mathbf{v}\cdot\nabla f(\mathbf{r},t).} \tag{4.3}$$

4.2 Hydrodynamic Equations

Fluid mechanics is based on the conservation of mass, energy and momentum. Mathematically we express this as conservation laws.

4.2.1 Conservation of mass

Considering a fixed volume element, let V denote the volume and S the area of the element, containing a fluid with density ρ. The mass is given by $M=\rho V$, therefore the rate of change in mass is

$$\frac{\partial M}{\partial t} \;=\; \frac{\partial}{\partial t}\int_V \rho dV. \tag{4.4}$$

If we have a system without sources and sinks, equation (4.4) must be equal to the outflow of mass across the surface per unit time. The flow out of a small surface element $d\mathbf{S}$ is $\rho\mathbf{v}\cdot d\mathbf{S}$. We integrate this expression over the surface of the element, S.

$$\int_S \rho\mathbf{v}\cdot d\mathbf{S} \;=\; \int_V \nabla\cdot(\rho\mathbf{v})dV, \tag{4.5}$$

where we used the divergence theorem. Now we see that equation (4.4) must be equal to (4.5), with a minus sign to compensate for the fact that we choose outward flow as positive flow,

$$\frac{\partial}{\partial t}\int_V \rho dV \;=\; -\int_V \nabla\cdot(\rho\mathbf{v})dV. \tag{4.6}$$

The choice of volume is arbitrary and equation (4.6) should hold for any volume, therefore the two integrands must be equal

$$\frac{\partial}{\partial t}\rho + \nabla\cdot(\rho\mathbf{v}) \;=\; 0. \tag{4.7}$$

This is the continuity equation in the Eulerian formulation.

4.2.2 Conservation of momentum

Consider a fluid element with volume V and density ρ. The element will feel pressure from the surrounding fluid as well as external forces. The net force acting on the fluid element in direction $\hat{\mathbf{n}}$ is given by

$$F_{\hat{\mathbf{n}}} = -\int_V \nabla\cdot(P\hat{\mathbf{n}})dV + F_{external}. \tag{4.8}$$

If there are no other external forces than gravity we can rewrite equation (4.8) as

$$F_{\hat{\mathbf{n}}} = -\int_V \nabla\cdot(P\hat{\mathbf{n}})dV + \int_V \rho\mathbf{g}\cdot\hat{\mathbf{n}}dV, \tag{4.9}$$

where $\mathbf{g} = -\nabla\Phi$ represents gravity. The rate of change in momentum must be equal to the net force acting on the fluid element. Equating the momentum change and the net force yields

$$\left(\frac{D}{Dt}\int_V \rho\mathbf{v}dV\right)\cdot\hat{\mathbf{n}} = -\int_V \nabla\cdot(P\hat{\mathbf{n}})dV + \int_V \rho\mathbf{g}\cdot\hat{\mathbf{n}}dV. \tag{4.10}$$

Here we have used the Lagrangian derivative since we are following a specific element. Taking the derivative under the integral on the left hand side gives:

$$\int_V \frac{D}{Dt}(\rho dV)\mathbf{v}\cdot\hat{\mathbf{n}} + \int_V \frac{D\mathbf{v}}{Dt}\rho dV\cdot\hat{\mathbf{n}} = -\int_V \nabla\cdot(P\hat{\mathbf{n}})dV + \int_V \rho\mathbf{g}\cdot\hat{\mathbf{n}}dV. \tag{4.11}$$

The first term on the left hand side is the change of mass in our fluid element. This term is zero due to mass conservation and equation (4.11) reduces to

$$\int_V \frac{D\mathbf{v}}{Dt}\rho dV\cdot\hat{\mathbf{n}} = -\int_V \nabla\cdot(P\hat{\mathbf{n}})dV + \int_V \rho\mathbf{g}\cdot\hat{\mathbf{n}}dV. \tag{4.12}$$

Equation (4.12) should hold for any volume and any direction, this implies that

$$\frac{D\mathbf{v}}{Dt}\rho = -\nabla P + \rho\mathbf{g}. \tag{4.13}$$

This is the momentum equation in the Lagrangian formalism. We can transform it into its Eulerian form by using the connection between Lagrangian and Eulerian derivatives, equation (4.3), we get:

$$\rho\frac{\partial \mathbf{v}}{\partial t} + \rho\mathbf{v}(\nabla\cdot\mathbf{v}) = -\nabla P + \rho\mathbf{g}. \tag{4.14}$$

4.2.3 Conservation of energy

Next we look at the energy of the system. We define

$$E = \rho\left(\frac{1}{2}v^2 + \Phi + \varepsilon\right), \tag{4.15}$$

where ε is specific internal energy and as before Φ represents gravity, as the total energy per unit volume. For an ideal gas, consisting of identical particles, ε is given by

$$\varepsilon = \frac{3}{2}\frac{k_B}{m}T, \tag{4.16}$$

where T is the temperature of the gas, k_B is Boltzmann's constant and m is the mass of the gas particles. Taking the Lagrangian derivative of E with respect to time gives

$$\begin{aligned}
\frac{DE}{Dt} &= \frac{\partial E}{\partial t} + \mathbf{v}\cdot\nabla E \\
&= \frac{D}{Dt}\left[\rho\left(\frac{1}{2}v^2 + \Phi + \varepsilon\right)\right] \\
&= \left[\frac{\partial \rho}{\partial t} + \mathbf{v}\cdot\nabla\rho\right]\frac{E}{\rho} + \rho\frac{D}{Dt}\left[\frac{1}{2}v^2 + \Phi + \varepsilon\right] \\
&= \left[\frac{\partial \rho}{\partial t} + \mathbf{v}\cdot\nabla\rho\right]\frac{E}{\rho} + \rho\left[\mathbf{v}\cdot\left(\frac{\partial \mathbf{v}}{\partial t} + \mathbf{v}(\nabla\cdot\mathbf{v})\right) + \frac{\partial \Phi}{\partial t} + \mathbf{v}\nabla\Phi + \frac{\partial \varepsilon}{\partial t} + \mathbf{v}\cdot\nabla\varepsilon\right].
\end{aligned}$$

Using equation (4.14) we can simplify this expression to

$$\frac{\partial E}{\partial t} + \mathbf{v}\cdot\nabla E + \mathbf{v}\cdot\nabla P = \left[\frac{\partial \rho}{\partial t} + \mathbf{v}\cdot\nabla\rho\right]\frac{E}{\rho} + \rho\frac{\partial \Phi}{\partial t} + \rho\left[\frac{\partial \varepsilon}{\partial t} + \mathbf{v}\cdot\nabla\varepsilon\right]. \tag{4.17}$$

Next we use equation (4.7) and the fact that $\nabla\cdot(\rho\mathbf{v}) = \rho\nabla\cdot\mathbf{v} + \mathbf{v}\cdot\nabla\rho$ to simplify the first term on the right hand side,

$$\frac{\partial E}{\partial t} + \mathbf{v}\cdot\nabla E + \mathbf{v}\cdot\nabla P = -(\rho\nabla\cdot\mathbf{v})\frac{E}{\rho} + \rho\frac{\partial \Phi}{\partial t} + \rho\frac{D\varepsilon}{Dt}. \tag{4.18}$$

Now we use the first law of thermodynamics $d\varepsilon = dQ - dW$, here dQ is the amount of heat energy deposited into a unit volume. We know that for a system without viscous effects $dW = -PdV$. Thus $d\varepsilon = dQ + PdV$ implying that

$$\frac{D\varepsilon}{Dt} = \frac{DQ}{Dt} + P\frac{D(1/\rho)}{Dt}, \tag{4.19}$$

where we have used that for specific volume $V = 1/\rho$. Note the mix of notation between thermodynamics and fluid mechanics. In thermodynamics there are no flows, to account for this we replace the derivatives with Lagrangian derivatives. Inserting equation (4.19) into (4.18) and rearranging gives

$$\frac{\partial E}{\partial t} + \mathbf{v} \cdot \nabla E + \mathbf{v} \cdot \nabla P + E \nabla \cdot \mathbf{v} = \rho \frac{\partial \Phi}{\partial t} + \rho \frac{dQ}{dt} - \frac{P}{\rho} \frac{d\rho}{dt}. \tag{4.20}$$

Now we just use equation (4.7) once more to rewrite the last term on the right hand side, after some rearranging we get

$$\frac{\partial E}{\partial t} + \nabla \cdot [(E + P)\mathbf{v}] = \rho \frac{\partial \Phi}{\partial t} + \rho \frac{DQ}{Dt}. \tag{4.21}$$

Arriving at the last equation in our set, the energy equation.

4.2.4 Conservation laws

We have now arrived at three governing equations, together with an equation of state they will fully describe our system.

$$\boxed{\begin{aligned} &\frac{\partial}{\partial t}\rho + \nabla \cdot (\rho \mathbf{v}) \ = \ 0, && \text{(4.22a)} \\ &\rho \frac{\partial \mathbf{v}}{\partial t} + \rho \mathbf{v} (\nabla \cdot \mathbf{v}) = -\nabla P + \rho \mathbf{g}, && \text{(4.22b)} \\ &\frac{\partial E}{\partial t} + \nabla \cdot [(E + P)\mathbf{v}] = \rho \frac{\partial \Phi}{\partial t} + \rho \frac{dQ}{dt}. && \text{(4.22c)} \end{aligned}}$$

4.2.5 Equation of state

As mentioned, an equation of state is needed to close up our system of equations. We can see this by looking at a simple case, assume that no heat is lost to the sorroudnings and that we can neglect gravity. In one spacial dimension we get

$$\begin{aligned} &\frac{\partial}{\partial t}\rho + \frac{\partial}{\partial x}\rho v = 0, \\ &\rho \frac{\partial v}{\partial t} + \rho v \frac{\partial}{\partial x} v = -\frac{\partial}{\partial x} P, \\ &\frac{\partial E}{\partial t} + \frac{\partial}{\partial x} \left[(E + P)v\right] = 0. \end{aligned}$$

We have four unknowns, (P, E, ρ, v), but only three equations. In order to solve the system we need a fourth equation. This fourth equation is supplied by the equation of state, which is determined by the properties of the fluid. In astrophysics its common to use the ideal gas approximation, with the following equation of state:

$$P = \rho k_B T. \tag{4.23}$$

In the case of an adiabatic process we can rewrite equation (4.23) as:

$$P = K\rho^{\gamma}, \tag{4.24}$$

here γ is a thermodynamic quantity related to the heat capacity, equal to $5/3$ for an ideal gas and K is a constant. See chapter 4 in [6].

It has been shown, experimentally, that the ideal gas approximation works very well for dilute gases. Most fluids in the astrophysical context have low density and as such the approximation will work very well.

4.3 Shocks

An important part of understanding the evolution of a supernova remnant is to describe the propagation of shocks trough the interstellar medium. Mechanical information propagates trough a fluid with the speed of sound, this means that a fluid can not adjust it self to perturbations faster than a sound wave can propagate trough it. If a perturbation is propagating trough the fluid faster than the speed of sound it will produce an discontinuous change at the point of the perturbation, a shock. In many astrophysical cases the density of the fluid is very low and thus the speed of sound is low, therefore shocks arise quite frequently.

4.3.1 Sound speed

Consider a uniform fluid in equilibrium and introduce a small perturbation

$$\rho = \rho_0 + \Delta\rho, \tag{4.25}$$
$$P = P_0 + \Delta P, \tag{4.26}$$
$$\mathbf{v} = \Delta\mathbf{v}. \tag{4.27}$$

It is important to note that these perturbations are for each individual fluid elements and as such are Lagrangian perturbations. For a uniform medium in equilibrium the Eulerian and Lagrangian perturbations are the same. However in more general cases this will not hold true. See chapter 6.1 and 6.2 in [6] for more details.

Returning to the case of a uniform medium, substituting the perturbation into (4.22a) and assuming that the perturbations are small yields

$$\rho_0 \nabla \cdot (\Delta\mathbf{v}) \ = -\frac{\partial}{\partial t}\Delta\rho. \tag{4.28}$$

Likewise substituting into (4.22b) and assuming no external forces gives

$$\rho_0 \frac{\partial \Delta\mathbf{v}}{\partial t} = -\nabla\Delta P. \tag{4.29}$$

Now let ∇ operate on equation (4.29) and $\frac{\partial}{\partial t}$ on equation (4.28)

$$\rho_0 \frac{\partial}{\partial t} \nabla \cdot (\Delta \mathbf{v}) \ = -\frac{\partial^2}{\partial t^2} \Delta \rho, \tag{4.30}$$

$$\rho_0 \nabla \frac{\partial \Delta \mathbf{v}}{\partial t} = -\nabla^2 \Delta P. \tag{4.31}$$

Combining equation (4.30) and equation (4.31) gives

$$\frac{\partial^2}{\partial t^2} \Delta \rho = \nabla^2 \Delta P, \tag{4.32}$$

$$\frac{\partial^2}{\partial t^2} \Delta \rho = \frac{dP}{d\rho} \nabla^2 \Delta \rho. \tag{4.33}$$

We recognize this as the wave equation,

$$\frac{\partial^2}{\partial t^2} \Delta \rho = c_s^2 \nabla^2 \Delta \rho,$$

where, $c_s = \sqrt{\frac{dP}{d\rho}}$ is the speed at which the wave propagates through the fluid. In the same fashion it is possible to derive the speed at which mechanical waves propagate in more general cases. The important concept is that the speed of sound is a finite number and a limit on how fast the medium can adjust to changes.

Note that the step from equation (4.32) to equation (4.33) implies a one to one relationship between pressure and density.

4.3.2 Rankine-Hugoniot conditions

Consider a one dimensional shock front, let $(\rho_2,\ v_2,\ P_2)$ be the density, velocity and pressure ahead of the shock and $(\rho_1,\ v_1,\ P_1)$ be the density, velocity and pressure behind the shock front. See figure 4.1.

In [6] a set of conditions are derived, called the Rankine-Hugoniot conditions, relating the post shocked medium to the unperturbed. In the rest frame of the shock they take the form:

$$\boxed{v_1 \rho_1 = v_2 \rho_2,} \tag{4.34}$$

$$\boxed{v_1^2 \rho_1 + P_1 = v_2^2 \rho_2 + P_2.} \tag{4.35}$$

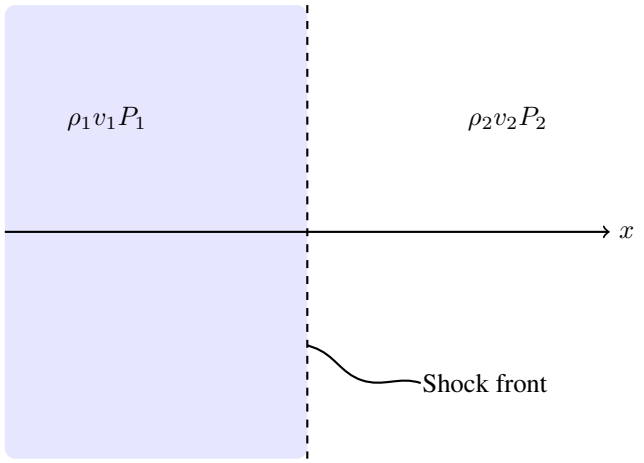

Figure 4.1: Shock front

4.3.3 Adiabatic shocks

Under the assumption that the system is adiabatic an additional condition can be derived.

$$\boxed{\frac{1}{2}v_1^2 + \varepsilon_1 + \frac{P_1}{\rho_1} = \frac{1}{2}v_2^2 + \varepsilon_2 + \frac{P_2}{\rho_2}.} \tag{4.36}$$

Furthermore under the this assumption it is possible to show that:

$$\frac{\rho_2}{\rho_1} = \frac{(\gamma-1)P_1 + (\gamma+1)P_2}{(\gamma-1)P_2 + (\gamma+1)P_1} = \frac{v_1}{v_2}. \tag{4.37}$$

To show this we first need an expression for the internal energy per unit mass. Starting from the first law of thermodynamics $d\varepsilon = dQ - dW$ and the adiabatic assumption, $dQ = 0$. Furthermore if there are no viscous forces then $dW = PdV$, this yields

$$\begin{aligned} d\varepsilon &= -PdV = P/\rho^2 d\rho = K\rho^{\gamma-2}d\rho, \\ \varepsilon &= \frac{P}{\rho}\frac{1}{\gamma-1}. \end{aligned} \tag{4.38}$$

In the second step we have used equation (4.23).

Inserting equation (4.38) into equation (4.36) gives

$$\frac{1}{2}v_1^2 + \frac{P_1}{\rho_1}\frac{1}{\gamma-1} + \frac{P_1}{\rho_1} = \frac{1}{2}v_2^2 + \frac{P_2}{\rho_2}\frac{1}{\gamma-1} + \frac{P_2}{\rho_2}. \tag{4.39}$$

Multiplying with $\rho_1^2\rho_2^2$ equation (4.39) becomes

$$\frac{1}{2}v_1^2\rho_1^2\rho_2^2 + \frac{P_1}{\rho_1}\frac{1}{\gamma-1}\rho_2^2\rho_1^2 + \frac{P_1}{\rho_1}\rho_2^2\rho_1^2 = \frac{1}{2}v_2^2\rho_1^2\rho_2^2 + \frac{P_2}{\rho_2}\frac{1}{\gamma-1}\rho_2^2\rho_1^2 + \frac{P_2}{\rho_2}\rho_2^2\rho_1^2. \tag{4.40}$$

Rewriting equation (4.35) as

$$\frac{v_1^2\rho_1^2}{\rho_1} + P_1 = \frac{v_2^2\rho_2^2}{\rho_2} + P_2 \tag{4.41}$$

and remembering that $v_1\rho_1 = v_2\rho_2$ gives

$$v_1^2\rho_1^2 = v_2^2\rho_2^2 = \frac{P_2 - P_1}{\rho_2 - \rho_1}\rho_1\rho_2. \tag{4.42}$$

Inserting equation (4.42) into equation (4.40) and rearranging gives

$$\frac{1}{2}\left(\rho_2^2 - \rho_1^2\right)\rho_1\rho_2\frac{P_2 - P_1}{\rho_2 - \rho_1} = \frac{\gamma}{\gamma - 1}\left(P_2\rho_1 - P_1\rho_2\right). \tag{4.43}$$

Simplifying this expression and collecting terms with ρ_1 and ρ_2 terms yields

$$\rho_2\left(\frac{1}{2}P_2 - \frac{1}{2}P_1 + \frac{\gamma}{\gamma - 1}P_1\right) = \rho_1\left(\frac{1}{2}P_1 - \frac{1}{2}P_2 + \frac{\gamma}{\gamma - 1}P_2\right), \tag{4.44}$$

implying that:

$$\frac{\rho_2}{\rho_1} = \frac{(\gamma - 1)P_1 + (\gamma + 1)P_2}{(\gamma - 1)P_2 + (\gamma + 1)P_1}.$$

Note that if the case of a strong shock, $\mathcal{M} \equiv v/c_s \gg 1$, equation (4.37) simplifies to

$$\frac{\rho_2}{\rho_1} = \frac{\gamma + 1}{\gamma - 1}. \tag{4.45}$$

For an adiabatic shock, $\gamma = 5/3$, this ratio is four. Thus there is an upper limit on how much a shock can compress the medium it passes trough. $\mathcal{M}$ is called the Mach number.

Chapter 5

Blast waves from supernovae

A simple way of looking at a supernova explosion is to say that a large amount of energy is released quasi instantaneously in to a star, ejecting mass into the interstellar medium. The mass ejected from the exploding star acts as a piston on the surrounding interstellar medium. Both the interstellar medium and the ejected material can have a complicated structure. In addition, the ejected material is often several orders of magnitude denser than the interstellar medium. As such the evolution of the remnant can be complicated, but in some very simplified cases it is possible to derive analytic solutions for the shock trajectory. However in more general cases we have to solve the system numerically.

The evolution of a supernova remnant is often divided into three stages: the ejecta dominated stage, the Sedov-Taylor stage and the radiation dominated stage. In the two first phases radiation does not play a significant roll in the dynamics, however in the last stage of the evolution radiation play a key roll. In the ejecta dominated stage the matter ejected from the exploding star still contain most of its initial energy and is expanding into the interstellar medium, with a speed much greater then the speed of sound. The ejected material is proceeded by a shock wave. This shock accelerates, heats and compresses the interstellar medium and as a result the shocked medium pushes back on the ejected material. A shock wave going backwards into the ejected material is created, often called the reverse shock.

As the ejected material moves further into the ambient medium it loses more and more of its energy. Radiation become important when most of the systems energy is contained in the shocked ambient medium. The transition stage between the radiation dominated stage and the ejected dominated stage is called the Sedov-Taylor stage. Since radiation is not the dominating factor in the dynamic during the ejected dominated stage and Sedov-Taylor stage it is a good approximation to neglect it.

5.1 Analytic solution

In 1999 Truelove and McKee[14] proposed a one dimensional solution for a supernova event surrounded by a uniform, cold and stationary medium. They also proposed solutions for ambient medium with a power law density. The structure of the ejected material is assumed to be a power law with power-law index n.

Uniform medium: Truelove and McKee proposed initial conditions which introduces three independence parameters: The ejected mass M_{ej}, total energy of the ejected mass E_{ej} and the density ρ_0 of the ambient medium. These parameters can be combined in a unique way to form characteristic length, time and mass scales:

$$\begin{aligned} R_{ch} &\equiv \left(\frac{M_{ej}}{\rho_0}\right)^{1/3}, \\ t_{ch} &\equiv \frac{M_{ej}^{5/6}}{E^{1/2}\rho_0^{1/3}}, \\ M_{ch} &\equiv M_{ej}. \end{aligned} \tag{5.1}$$

Note that these characteristic scales gives the scales for parameters like velocity and density. Defining a new set of dimensionless variables,

$$\begin{aligned} r &\equiv R_p/R_{ch}, \\ t &\equiv t_p/t_{ch}, \\ m &\equiv M_p/M_{ch}, \end{aligned} \tag{5.2}$$

here R_p, t_p and M_p are the physical quantities.

For an uniformly distributed ejecta, $n = 0$, the solutions for the forward shock in the ejected dominated stage are given by

$$\begin{aligned} r_b &= 2.01t(1 + 1.72t^{3/2})^{-2/3}, \\ v_b &= 2.01(1 + 1.72t^{3/2})^{-5/3}. \end{aligned} \tag{5.3}$$

In the Sedov-Taylor stage we get the following solutions

$$\begin{aligned} r_b &= 2.01t(1.42t - 0.254)^{2/5}, \\ v_b &= 0.568(1.42t - 0.254)^{-3/5}. \end{aligned} \tag{5.4}$$

Here r_b and v_b are the position and velocity of the forward shock created by the supernova. A detailed discussion can be found in [14]. Solutions for a more general ejecta structure are also given.

Power law medium: If the medium has a power law distribution, in other words $\rho \propto r^{-s}$, the characteristic scales are:

$$\begin{aligned} R_{ch} &\equiv M_{ej}^{1/(3-s)} K^{-1/(3-s)}, \\ t_{ch} &\equiv \frac{M_{ej}^{(5-s)/2(3-s)} K^{-1/(3-s)}}{E^{1/2}}, \\ M_{ch} &\equiv M_{ej}. \end{aligned} \tag{5.5}$$

As in the uniform case they define a set of new dimensionless variables. An interesting case is when $s = 2$, emulating the distribution created by stellar wind. In this case the solution for the ejecta dominated stage are given by

$$\begin{aligned} t(R_b) &= 0.594 \left(\frac{3}{5}\right)^{1/2} R_b \left[1 - 1.50(3R_b)^{1/2}\right]^{-2/3}, \\ v_b(R_b) &= 1.68 \left(\frac{3}{5}\right)^{1/2} \frac{1 - 1.50(3R_b)}{1 - (3R_b)^{1/2}}. \end{aligned} \tag{5.6}$$

See Appendix A in [14] for details and solutions for $s \neq 2$.

Chapter 6

Numerical method

Our ability to solve the evolution of a supernova remnant analytically is limited to the simple cases where strong assumptions have been made on the structure of both the ejected material and the ambient medium surrounding the star. In particular, one has to assume spherical symmetry. An other approach is to solve the system numerically. The problem at hand is discontinuous and we have to solve a set of five coupled differential equations simultaneously, equations (4.22) and an equation of state.

Finite differentiating schemes work relatively well with smooth flows, but in the case of a supernova remnant we have a discontinuity at the shock and one at the contact surface between the ejecta and ambiance material. The discontinuity at the contact surface is an issue for grid resolution. For example: If we measure the temperature on the north and south pole it would be a bad approximation to say that the temperature on the equator is half way between the two. In the same way it is important to make sure that abrupt changes are resolved on the grid. We have to handle the discontinuity created by shock more carefully. See chapter 6.1 in [3].

There are several ways to handle shocks on a grid. Riemann solvers are well known and accurate solutions, however they are notoriously complex and difficult to work with. A simpler method is to introduce what is known as artificial viscosity.

6.1 Discretization

In the Lagrangian formulation of equations (4.22) all nonlinear terms disappear thus making it easier to work with. In one dimension a grid solution can be utilized without worrying about deformation of the grid and resulting accuracy issues, see [2]. Therefore, if the problem is spherical symmetry, it is advantageous to transform our coordinates into

spherical coordinates making the problem one dimensional in space.

6.1.1 Lagrangian formulation

The Lagrangian form of (4.22) is

$$\frac{D\rho}{Dt} + \rho\nabla \cdot \mathbf{v} = 0, \tag{6.1}$$
$$\frac{D\mathbf{v}}{Dt}\rho = -\nabla P, \tag{6.2}$$
$$\frac{D\varepsilon}{Dt} - \frac{P}{\rho^2}\frac{D\rho}{Dt} = 0, \tag{6.3}$$

where in the last equation the variable has been recast into specific internal energy, ε. Note that we have neglected gravity and assumed an adiabatic process.

In the Lagrangian formulation we attach a coordinate system to a given fluid element and follow it trough the flow, and as such its convenient to choose mass as the free variable instead of position. In spherical coordinates the two are related by

$$M = \frac{4\pi}{3}\rho r^3. \tag{6.4}$$

Taking the Lagrangian derivative with respect to r on both sides gives

$$Dm = 4\pi\rho r^2 Dr. \tag{6.5}$$

As such we can rewrite equations (6.1)-(6.3) as:

$$4\pi r^2 \frac{Dr}{Dm} = 1/\rho, \tag{6.6}$$
$$\frac{Dv}{Dt} = -4\pi r^2 \frac{DP}{Dm}, \tag{6.7}$$
$$\frac{D\varepsilon}{Dt} = -4\pi P \frac{D}{Dm}(r^2 v), \tag{6.8}$$
$$\frac{Dr}{Dt} = v, \tag{6.9}$$

for a spherical symmetric system. Together with the equation of state,

$$P = (\gamma - 1)\rho\varepsilon, \tag{6.10}$$

we have five unknowns and five equations.

6.1.2 Finite differencing

The discretization of these five equations will follow the approach in [2]: Set up a staggered grid, use finite differencing and employ artificial viscosity to handle the shocks.

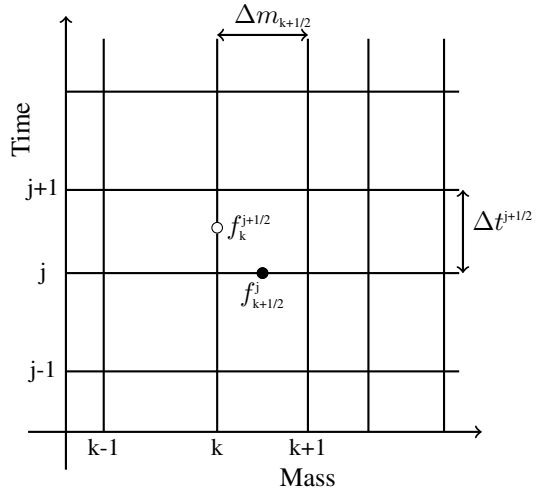

Figure 6.1: Staggerd grid

We defined indices as shown in figure 6.1, here f represents a function we are interested in. We set up the grid so that density, pressure, specific internal energy and mass, ($\rho^{j}_{k+1/2}$, $P^{j}_{k+1/2}$, $\varepsilon^{j}_{k+1/2}$, $m^{j}_{k+1/2}$) are defined at at the center of vertical cell edges. While the velocity $v^{j+1/2}_{k}$ is defined at horizontal cell edges and radius the r^{j}_{k} at cell corners.

In spherical coordinates the mass elements are given by:

$$\Delta m_{k+1/2} = \frac{4\pi}{3}\left[(r^0_{k+1})^3 - (r^0_k)^3\right]\rho^0_{k+1/2}. \tag{6.11}$$

We integrate equation (6.7) over a cell centered around k

$$\int_{\Delta m_k} \frac{Dv}{Dt} dm = -\int_{\Delta m_k} \frac{DP}{Dm} 4\pi r^2 dm.$$

$$\int_{k-1/2}^{k+1/2} \frac{Dv}{Dt} dm = -\int_{k-1/2}^{k+1/2} \frac{DP}{Dm} 4\pi r^2 dm. \tag{6.12}$$

By approximating the acceleration to be constant over the small time interval we get:

$$\frac{v^{j+1/2}_k - v^{j-1/2}_k}{\Delta t^j}\Delta m_k = -4\pi (r^j_k)^2\left[P^j_{k+1/2} - P^j_{k-1/2}\right]. \tag{6.13}$$

Solving for $v^{j+1/2}_k$ yields

$$v^{j+1/2}_k = v^{j-1/2}_k - 4\pi (r^j_k)^2 \frac{P^j_{k+1/2} - P^j_{k-1/2}}{\Delta m_k}\Delta t^j. \tag{6.14}$$

Note that:

$$\Delta t^{j} = \frac{1}{2}(\Delta t^{j+1/2} + \Delta t^{j-1/2})$$

and

$$\Delta m_{k} = \frac{1}{2}(\Delta m_{k+1/2} + \Delta m_{k-1/2}).$$

After calculating the velocity we can use equation (6.9) to update the position r_k of cell k:

$$\begin{aligned} \frac{Dr}{Dt} &= v_{k}^{j+1/2} = \frac{r_{k}^{j+1} - r_{k}^{j}}{\Delta t^{j}}, \\ r_{k}^{j+1} &= r_{k}^{j} + v_{k}^{j+1/2}\Delta t^{j}. \end{aligned} \tag{6.15}$$

By definition the mass of a given element should be constant in the Lagrangian formulation, therefore the change in volume of an element can directly be translated into a change in density. For a given cell that mass is simply the density times the volume:

$$\Delta m_{k+1/2} = V_{k+1/2}^{j+1}\rho_{k+1/2}^{j+1}, \tag{6.16}$$

where the volume is given by

$$V_{k+1/2}^{j+1} = \frac{4\pi}{3}\left[(r_{k+1}^{j+1})^3 - (r_{k}^{j+1})^3\right]. \tag{6.17}$$

Combining equation (6.16) and equation (6.17) yields

$$\rho_{k+1/2}^{j+1} = \frac{3}{4\pi}\frac{\Delta m_{k+1/2}}{[(r_{k+1}^{j+1})^3 - (r_{k}^{j+1})^3]}. \tag{6.18}$$

Next we look at the energy equation. On the grid shown in figure 6.1 equation (6.8) is given by:

$$\frac{D\varepsilon}{Dt} = \left[-4\pi P\frac{D}{Dm}(r^2 v)\right]_{j+1/2}. \tag{6.19}$$

Integrating this equation over a mass element centered at $k + 1/2$ yields

$$\frac{D\varepsilon}{Dt}\Delta m_{k+1/2} = -4\pi P_{k-1/2}^{j+1/2}[(r_{k+1}^{j+1/2})^2 v_{k+1}^{j+1/2} - (r_{k}^{j+1/2})^2 v_{k}^{j+1/2}]. \tag{6.20}$$

As such we get

$$\frac{\varepsilon_{k+1/2}^{j+1} - \varepsilon_{k+1/2}^{j}}{\Delta t^{j+1/2}}\Delta m_{k+1/2} = -4\pi P_{k+1/2}^{j+1/2}[(r_{k+1}^{j+1/2})^2 v_{k+1}^{j+1/2} - (r_{k}^{j+1/2})^2 v_{k}^{j+1/2}], \tag{6.21}$$

$$\varepsilon_{k+1/2}^{j+1} = \varepsilon_{k+1/2}^{j} - 4\pi P_{k+1/2}^{j+1/2}\frac{[(r_{k+1}^{j+1/2})^2 v_{k+1}^{j+1/2} - (r_{k}^{j+1/2})^2 v_{k}^{j+1/2}]}{\Delta m_{k+1/2}}\Delta t^{j+1/2}. \tag{6.22}$$

To evaluate the right hand side of equation (6.22) we need an expression for the pressure at half time steps,

$$P_{k+1/2}^{j+1/2} = \frac{1}{2}(P_{k+1/2}^{j+1} + P_{k+1/2}^{j}).$$

However P^{j+1} depends on ε^{j+1} and we are back at the start. We could try to approximate $P^{j+1/2}$ using only P^j, but in doing so the scheme would be reduced to first order and problems would arise if the energy is sensitive to changes in pressure.

There are several ways to solve this problems, we will use a method that does not depend on the equation of sate. First approximate $P^{j+1/2}$ using P^j, finding an approximate value for ε^{j+1} and then approximating P^{j+1} with the equation of state. Now we can use the approximated value for P^{j+1} to find the value of ε^{j+1} and then update the pressure with the equation of state.

6.1.3 Artificial viscosity

Physically a shock is very thin and this is problematic to model on a grid. We will use artificial viscosity to handle the shock related problems. The idea is to make the flow more diffusive and effectively broadening the shock, spreading it out over several grid cells. This is purely a numerical trick and we only want to apply it near the shock and as such we have some freedom in selecting the implementation of the dissipative effects. We only require that it gives the right jump conditions, only affects the flow near the shock and do not broaden the shock to much.

In 1950 von Neumann and Richtmyer showed that, for a slab symmetric system, adding an artificial pressure term fulfills the requirements if the pressure term is given by

$$Q = \begin{cases} q^2(\Delta x)^2 \rho \left|\frac{\partial v}{\partial x}\right|^2, & \frac{\partial v}{\partial x} < 0 \\ 0, & \frac{\partial v}{\partial x} > 0 \end{cases}, \tag{6.23}$$

see [15]. This method was shown to work well in Cartesian coordinates, but it was found that problems arise in spherical coordinates. See chapter 6.1.4 in [3] for details.

To gain some insight into how we can implement a better artificial viscosity, it is a good idea to look at the equation governing a real viscous fluid: The Navier-Stokes equation, if we include shear viscosity and neglect gravity is given by

$$\frac{\partial \mathbf{v}}{\partial t} + \mathbf{v} \cdot \nabla \mathbf{v} = -\frac{1}{\rho}\nabla P + \frac{\eta}{\rho}\left[\nabla^2 \mathbf{v} + \frac{1}{3}\nabla(\nabla \cdot \mathbf{v})\right], \tag{6.24}$$

see chapter 11.2 in [6].

Concentrating on the viscosity term and making a coordinate transformation into spherical coordinates yields

$$\frac{1}{r^3}\frac{\partial}{\partial r}\left(r^3 \eta \left[\frac{\partial v}{\partial r} - \frac{1}{3}\nabla \cdot \mathbf{v}\right]\right).$$

From this expression we can define the viscous pressure:

$$P_{vis} \equiv \eta \left[\frac{\partial v}{\partial r} - \frac{1}{3}\nabla \cdot \mathbf{v}\right]. \tag{6.25}$$

It is important to note that the above discussion is valid for a fluid where physical viscosity is important. However it is only interesting in the current case as a guide for constructing an artificial viscosity term. Recalling the idea of von Neumann and Richtmyer, we introduce an artificial pressure term:

$$Q \equiv -\xi \left[\frac{\partial v}{\partial r} - \frac{1}{3} \nabla \cdot \mathbf{v} \right] = -\xi \frac{2}{3} r \frac{\partial}{\partial r} \left(\frac{v}{r} \right), \tag{6.26}$$

where ξ is the artificial viscosity coefficient that we will define later.

Centering: Keeping with the notion of introducing artificial viscosity into the numerical scheme as a pressure term, it seems natural to define it at the same grid points as the real pressure,

$$Q \propto \frac{v_{\mathrm{k+1}} - v_{\mathrm{k}}}{r_{\mathrm{k+1}} - r_{\mathrm{k}}} - \frac{v_{\mathrm{k+1}} + v_{\mathrm{k}}}{r_{\mathrm{k+1}} + r_{\mathrm{k}}}. \tag{6.27}$$

However with this definition we see that $Q = 0$ at the first grid cell, $r_1 = v_1 = 0$. To avoid this problem W.Benz[2] proposes to consider the volume average of $\nabla \cdot \mathbf{v}$ and $\frac{\partial v}{\partial r}$. They are given by:

$$\begin{aligned} \overline{\nabla \cdot \mathbf{v}} &= \frac{1}{\Delta V_{\mathrm{k+1/2}}} \int_{\Delta V_{\mathrm{k+1/2}}} \nabla \cdot \mathbf{v} dV \frac{4\pi}{\Delta V_{\mathrm{k+1/2}}} \int_{\Delta V_{\mathrm{k+1/2}}} \frac{\partial}{\partial r} (r^2 v) dr, \\ &= 4\pi \frac{(r_{\mathrm{k+1}})^2 v_{\mathrm{k+1}} - (r_{\mathrm{k}})^2 v_{\mathrm{k}}}{\Delta V_{\mathrm{k+1/2}}} \end{aligned} \tag{6.28}$$

and

$$\overline{\frac{\partial v}{\partial r}} = \frac{1}{\Delta V_{\mathrm{k+1/2}}} \int_{\Delta V_{\mathrm{k+1/2}}} \frac{\partial v}{\partial r} dV \pi (r_{\mathrm{k+1/2}})^2 \frac{v_{\mathrm{k+1}} - v_{\mathrm{k}}}{\Delta V_{\mathrm{k+1/2}}}. \tag{6.29}$$

$\Delta V_{\mathrm{k+1/2}}$ is found by differentiating the volume element with respect to r:

$$\frac{DV}{Dr} = \frac{D}{Dr} \left(\frac{4\pi}{3} r^3 \right) = 4\pi r^2. \tag{6.30}$$

Implying that

$$\Delta V = 4\pi r^2 \Delta r. \tag{6.31}$$

Inserting equation (6.28) and (6.29) into equation (6.26) yields:

$$\begin{aligned} Q^{\mathrm{j+1/2}}_{\mathrm{k+1/2}} &= \xi^{\mathrm{j+1/2}}_{\mathrm{k+1/2}} \left[4\pi (r^{\mathrm{j+1/2}}_{\mathrm{k+1/2}})^2 \frac{v^{\mathrm{j+1/2}}_{\mathrm{k+1}} - v^{\mathrm{j+1/2}}_{\mathrm{k}}}{\Delta V^{\mathrm{j+1/2}}_{\mathrm{k+1/2}}} - \frac{1}{3} 4\pi \frac{(r^{\mathrm{j+1/2}}_{\mathrm{k+1}})^2 v^{\mathrm{j+1/2}}_{\mathrm{k+1}} - (r^{\mathrm{j+1/2}}_{\mathrm{k}})^2 v^{\mathrm{j+1/2}}_{\mathrm{k}}}{\Delta V^{\mathrm{j+1/2}}_{\mathrm{k+1/2}}} \right] \\ &= \frac{\xi^{\mathrm{j+1/2}}_{\mathrm{k+1/2}}}{\Delta r^{\mathrm{j+1/2}}_{\mathrm{k+1/2}}} \left[v^{\mathrm{j+1/2}}_{\mathrm{k+1}} - v^{\mathrm{j+1/2}}_{\mathrm{k}} - \frac{1}{3} \frac{(r^{\mathrm{j+1/2}}_{\mathrm{k+1}})^2 v^{\mathrm{j+1/2}}_{\mathrm{k+1}} - (r^{\mathrm{j+1/2}}_{\mathrm{k}})^2 v^{\mathrm{j+1/2}}_{\mathrm{k}}}{(r^{\mathrm{j+1/2}}_{\mathrm{k+1/2}})^2} \right] \\ &= \frac{\xi^{\mathrm{j+1/2}}_{\mathrm{k+1/2}}}{\Delta r^{\mathrm{j+1/2}}_{\mathrm{k+1/2}}} \left[v^{\mathrm{j+1/2}}_{\mathrm{k+1}} \left(1 - \frac{1}{3} \left[\frac{r^{\mathrm{j+1/2}}_{\mathrm{k+1}}}{r^{\mathrm{j+1/2}}_{\mathrm{k+1/2}}} \right]^2 \right) - v^{\mathrm{j+1/2}}_{\mathrm{k}} \left(1 - \frac{1}{3} \left[\frac{r^{\mathrm{j+1/2}}_{\mathrm{k}}}{r^{\mathrm{j+1/2}}_{\mathrm{k+1/2}}} \right]^2 \right) \right]. \end{aligned} \tag{6.32}$$

As mentioned before, there is some freedom to chose the implementation of artificial viscosity. The form of Q, up to the factor ξ, was decided by comparing it to the physical properties of viscous fluids. Determining ξ is purely a numerical issue and success of simulations is the only judge. However dimensional analysis can give some restrictions.

$$[\text{pressure}] = \frac{\text{kg}}{\text{s}^2\text{m}} \Rightarrow [\xi] = \frac{\text{kg}}{\text{ms}}.$$

Further more equation (6.32) should reduce to the original expression, given by von Neumann and Richtmyer, for slab symmetry. Both these criteria are fulfilled if

$$\xi^{j+1/2}_{k+1/2} = -q^2 \rho^{j+1/2}_{k+1/2} \left| v^{j+1/2}_{k+1} - v^{j+1/2}_{k} \right| \Delta r^{j+1/2}_{k+1/2}, \tag{6.33}$$

see chapter 4.4 in [4].

Inserting this expression into equation (6.32) yields:

$$\begin{aligned} Q = & -q^2 \rho^{j+1/2}_{k+1/2} \left| v^{j+1/2}_{k+1} - v^{j+1/2}_{k} \right| \\ & \times \left[v^{j+1/2}_{k+1} \left(1 - \frac{1}{3} \left[\frac{r^{j+1/2}_{k+1}}{r^{j+1/2}_{k+1/2}} \right]^2 \right) - v^{j+1/2}_{k} \left(1 - \frac{1}{3} \left[\frac{r^{j+1/2}_{k}}{r^{j+1/2}_{k+1/2}} \right]^2 \right) \right], \end{aligned} \tag{6.34}$$

where q is a constant that has to be determined by numerical experiments.

The final discrete equations are found by adding the artificial pressure term to our system, as dictated by the energy and momentum equation for a viscid fluid. The derivation follows along the lines of the discussion for non viscid fluids, the resulting equations are:

$$\begin{aligned} v^{j+1/2}_{k} = & \, v^{j-1/2}_{k} - A^{j}_{k} \frac{P^{j}_{k+1/2} - P^{j}_{k-1/2}}{\Delta m_k} \Delta t^{j} \\ & - \frac{1}{2} \left[Q^{j-1/2}_{k+1/2} (3A^{j}_{k+1/2} - A^{j}_{k}) - Q^{j-1/2}_{k-1/2} (3A^{j}_{k+1/2} - A^{j}_{k}) \right] \frac{\Delta t^{j}}{\Delta m_k} \end{aligned} \tag{6.35}$$

$$\begin{aligned} \varepsilon^{j+1}_{k+1/2} = & \, \varepsilon^{j}_{k+1/2} \\ & - P^{j+1/2}_{k+1/2} \frac{\left[A^{j+1/2}_{k+1} v^{j+1/2}_{k+1} - A^{j+1/2}_{k} v^{j+1/2}_{k} \right]}{\Delta m_{k+1/2}} \Delta t^{j+1/2} \\ & - \frac{1}{2} Q^{j+1/2}_{k+1/2} \left[v^{j+1/2}_{k+1} (3A^{j+1/2}_{k+1/2} - A^{j+1/2}_{k+1}) - v^{j+1/2}_{k} (3A^{j+1/2}_{k+1/2} - A^{j+1/2}_{k}) \right] \frac{\Delta t^{j+1/2}}{\Delta m_{k+1/2}} \end{aligned} \tag{6.36}$$

$$\rho^{j+1}_{k+1/2} = \frac{3}{4\pi} \frac{\Delta m_{k+1/2}}{\left[(r^{j+1}_{k+1})^3 - (r^{j+1}_{k})^3 \right]}$$

$$r^{j+1}_{k} = r^{j}_{k} + v^{j+1/2}_{k} \Delta t^{j}. \tag{6.37}$$

Here A^{j}_{k} has been introduced to reduce clutter. It is defined as follows:

$$A^{j}_{k} = 4\pi (r^{j}_{k})^2.$$

In the case of an adiabatic process these four equations are supplemented with the discrete version of the equation of state:

$$P^{j+1/2}_{k+1/2} = \frac{1}{2} (\gamma - 1) \rho^{j+1/2}_{k+1/2} (\varepsilon^{j+1}_{k+1/2} + \varepsilon^{j}_{k+1/2}). \tag{6.38}$$

6.2 Analyzing numerical results

When we solve differential equations numerically it is done by solving dimensionless equations, often rescaled in some way, and we need to understand what the numbers mean. If the algorithm tells us that $x = 3$ we need to understand the physical meaning. One way to do this is to just plug our numbers into the machine as they are. Consider the example of a ball failing being dropped from 10 meters with zero initial velocity,

$$x = 10.0\mathrm{m} - \frac{1}{2}9.81\frac{\mathrm{m}}{\mathrm{s}^2} \cdot t^2.$$

Here we can simply say that $x' = \frac{x}{m}$ and $t' = \frac{t}{s}$. We now have dimensionless equation, to plug into the computer and if the program returns $x' = 3$ we know that to recover the physics we just multiply by one meter. This method works well when dealing with numbers that are not to small or not to large, but once we start dealing with more complex problems it is often convenient to rescale the equations. For the above example $x' = \frac{\mathrm{x}}{10\mathrm{m}}$ and $t' = \frac{t}{\mathrm{s}}$, would be a good scale. Resulting in

$$x' = 1 - \frac{1}{2}0.981t'^2. \tag{6.39}$$

When rescaling it is important to be careful, to make sure that the scales agree with each other. We can for example not rescale time by a factor four, length by a factor five and velocity by a factor eight. Since [velocity] = [length]/[time] it must scale as four divided by five.

Example: A one-dimensional simple harmonic oscillator is described by

$$\ddot{x} + \omega^2 x = 0.$$

If we do dimensional analysis it is clear that $[\omega] = 1/\mathrm{s}$. So by choosing a timescale we also choose a scale for ω. We can choose our rescaling such that,

$$t' = \frac{t}{t_s} = \frac{t}{1/\omega} = t \cdot \omega$$

$$x' = \frac{x}{x_s}.$$

Now we only need to rescale $\ddot{x}$, but since we already have fixed a scale for length it is fixed.

$$\ddot{x}' = \frac{d^2x'}{dt'^2} = \frac{d^2x}{dt^2} \cdot \frac{t_s^2}{x_s} = \frac{d^2x}{dt^2}\frac{1}{x_s\omega^2}.$$

This yields the following dimensionless equation for our harmonic oscillator

$$\ddot{x}' \cdot (x_s\omega^2) + \omega^2 x' \cdot x_s = \ddot{x}' + x' = 0.$$

Now we see why it was smart to choose the time scale to be the inverse of ω.

As seen in the above discussion it is possible to define scales from initial conditions and from parameters in the equations. For a supernova event it can be convenient to let the initial values of the surrounding medium define scales. Let ε_0 and ρ_0 denote the initial internal specific energy and density. Furthermore let R_0 denote the size of the grid, in other words the spatial boundary of the simulation. Choosing a scale where,

$$1 = \varepsilon_0 = \rho_0 = R_0$$

and remembering that,

$$\begin{aligned}[\varepsilon] &= \mathrm{m/s^2} \\ [\rho] &= \mathrm{kg/m^3} \\ [r] &= \mathrm{m},\end{aligned}$$

results in the following rescaling:

$$\begin{aligned}&\varepsilon' = \frac{\varepsilon}{\varepsilon_0}, \rho' = \frac{\rho}{\rho_0}, r' = R/R_0, \\ &t' = \frac{R_0}{\sqrt{\varepsilon_0}} \text{ and } m' = \rho_0 R_0^3.\end{aligned}$$

One should note that equations (6.35) do not contain any coefficients with dimension, as such the equations them self will be unchanged by the choice of scale and we only need to worry about rescaling the initial values.

Chapter 7

Numerical simulations

The numerical equations found in chapter 6 can be used to model the evolution of a supernova remnant, assuming that the problem is spherical symmetric. Initial values are chosen to mimic real astrophysical conditions, however the main focus is given to investigating the general evolution and less attention is paid to tune initial values to exactly fit observed events. This gives an idea of the evolution, while more accurate results require more complex models. Note that initial values have to be specified every grid point.

Several density profiles for the ambient medium surrounding the star are investigated, and when possible numerical results are compared to analytic solutions. The analytic shock trajectories were used as a test for our numerical results. If the simulations produce results that agree with analytic solutions, in the relative simple cases where they can be found, we might expect them to produce good results for more complex cases.

7.1 The model

The supernova explosion is modelled as an injection of thermal energy, E_s, into a cold sphere with mass M_s, radius R_s and constant density ρ_s, surrounded by a medium with density $\rho_a = \rho(r)$ and temperature $T_a = T(r)$. Truelove and McKee investigate ejected material with a given mass and kinetic energy expanding into an ambient medium. They assume that the ejected material expands freely for a short time, t_0, the radius of the outer most ejecta is given by

$$R = v_{ej} t_0, \tag{7.1}$$

where v_{ej} is connected to the kinetic energy of the ejected material as follows:

$$E = \frac{3}{5}\frac{1}{2} M v_{ej}^2, \tag{7.2}$$

if the mass and kinetic energy of the ejected material is M and E, and the density of the ejecta is constant, see [14]. Solving for R yields

$$R(E, M) = t_0 \times \left[\frac{10E}{3M}\right]^{1/2}. \tag{7.3}$$

The expansion into the ambient medium is assumed to be adiabatic and both the ejected material and the ambient medium is modelled as ideal gas consisting of hydrogen.

7.2 Results

The results are given as plots showing the time evolution of the system, plotting pressure, density and velocity in the same graph. Initial conditions are presented as a plot of the initial density profile of the ambient medium together with a table listing M_s, R_s, T_a and t_0. The density of the ambient medium at $\rho_a(r)$ is also listed, as well as the total mass of the ambient medium M_a. Lastly the size of the grid R_{max} is also listed, in other words the outer spatial boundary of the simulations. The values in both SI and CGS unites are included for the readers conveniences.

The trajectory of the forward shock is also presented, together with analytically solutions when relevant.

7.3 Constant density

The first case that was investigated was a supernova surrounded by a medium with constant density.

M_s	E_s	R_s	T_a
$5M_\odot$	1×10^{44} J	0.144 pc	10K
9.95×10^{33} g	1×10^{52} erg	4.44×10^{17} cm	10K
$\rho_a(r)$	Grid size	t_0	M_a
$1.67 \times 10^{-21}\mathrm{kg/m^3}$	10 pc	1 yr	$103.3\mathrm{M}_\odot$
$1.67 \times 10^{-24}\mathrm{g/cm^3}$	3.085×10^{19} cm	31 556 926 s	2.05×10^{35} g

The shock trajectory was compared to the analytically solution and found to agree well. See figure 7.1. Figure 7.2 and 7.3 shows the pressure, density and radial velocity at different times. $(P,\ \rho,\ v)$ The scales are given for velocity, density and pressure are given by:

$$v_s = 9.39 \times 10^5 \text{ m/s} = 9.39 \times 10^7 \text{ cm/s}$$
$$\rho_s = 1.67 \times 10^{-19} \text{ kg/m}^3 = 1.67 \times 10^{-22} \text{ g/cm}^3$$
$$P_s = 1.84 \text{ Pa} = 18.4 \text{ Ba}$$

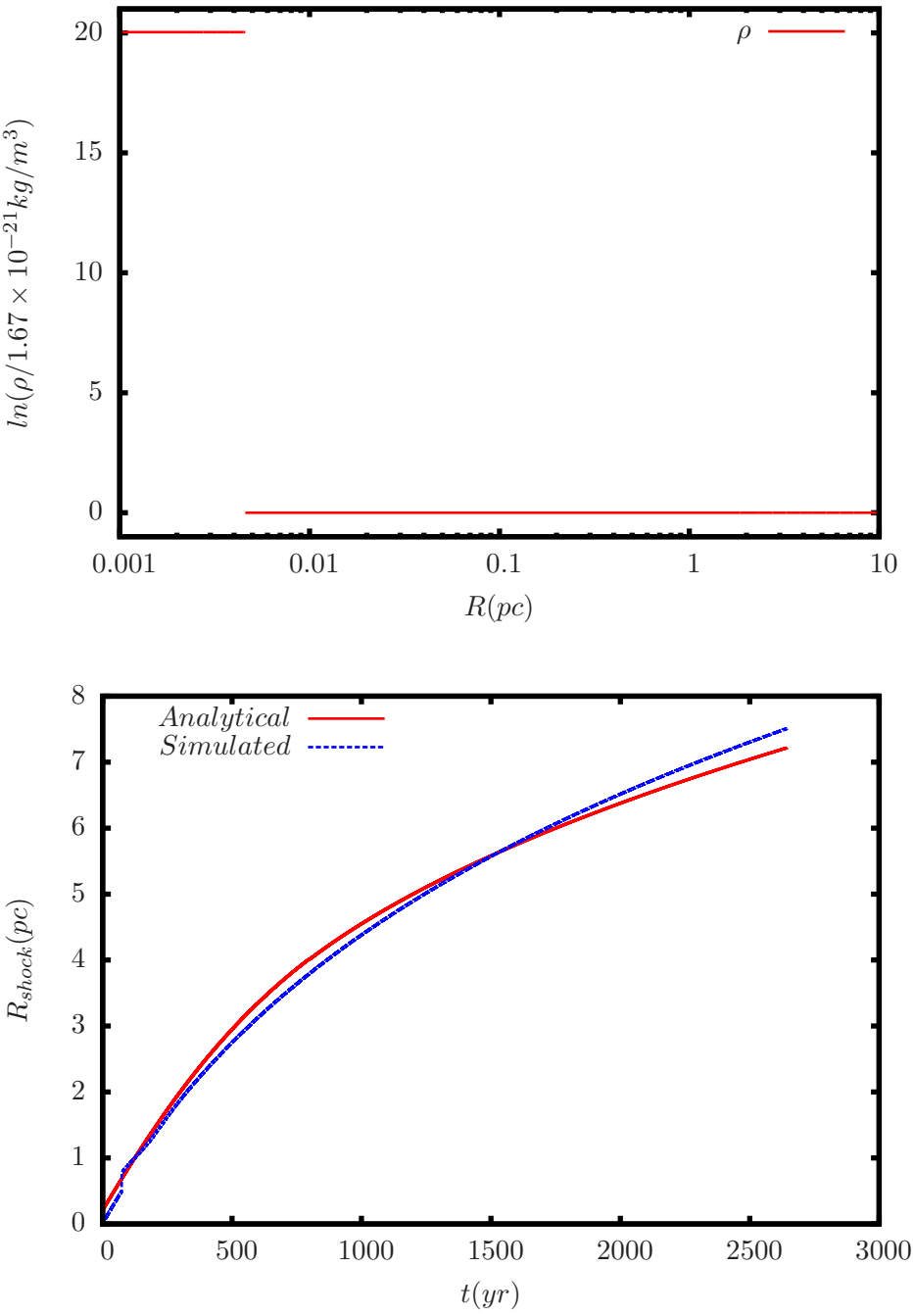

Figure 7.1: Density distribution and Shock trajectory

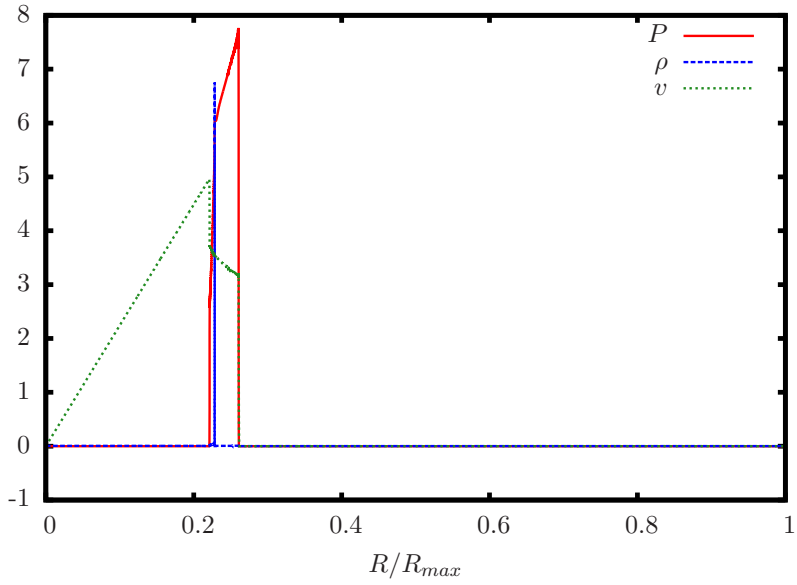

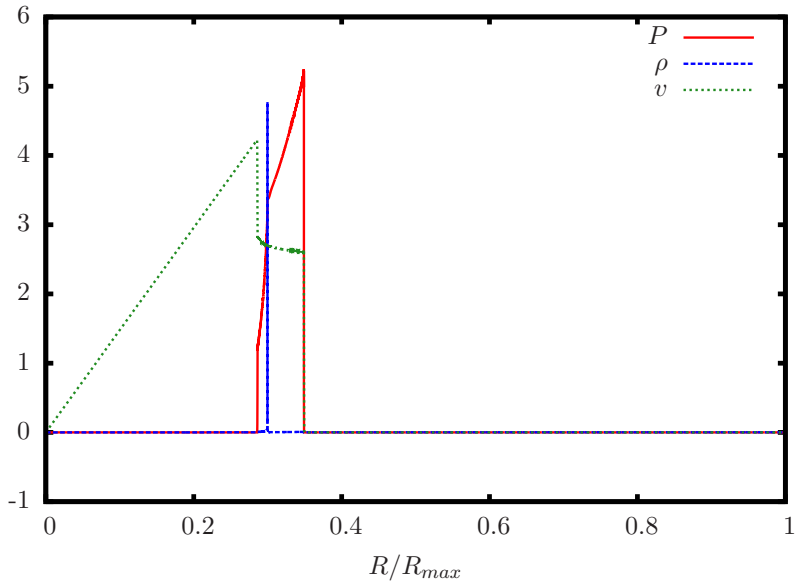

Figure 7.2: Pressure, density and velocity at t = 438.38 yr and t = 677.03 yr

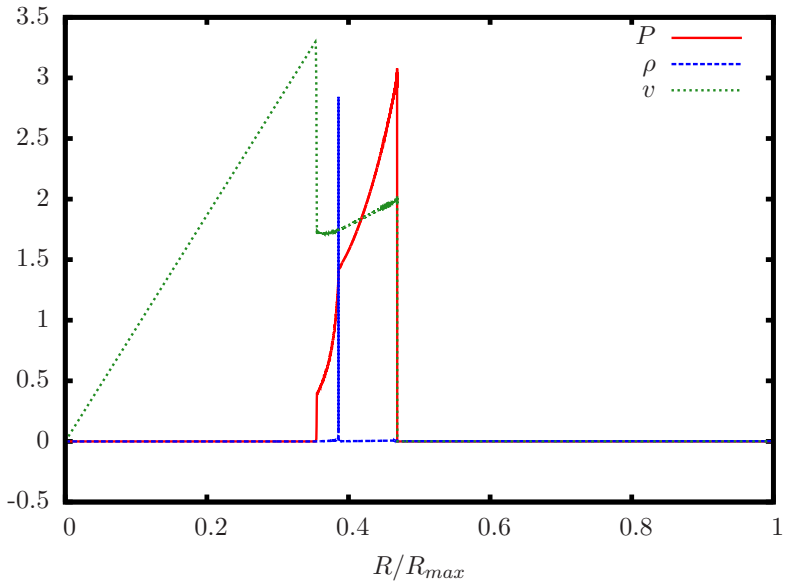

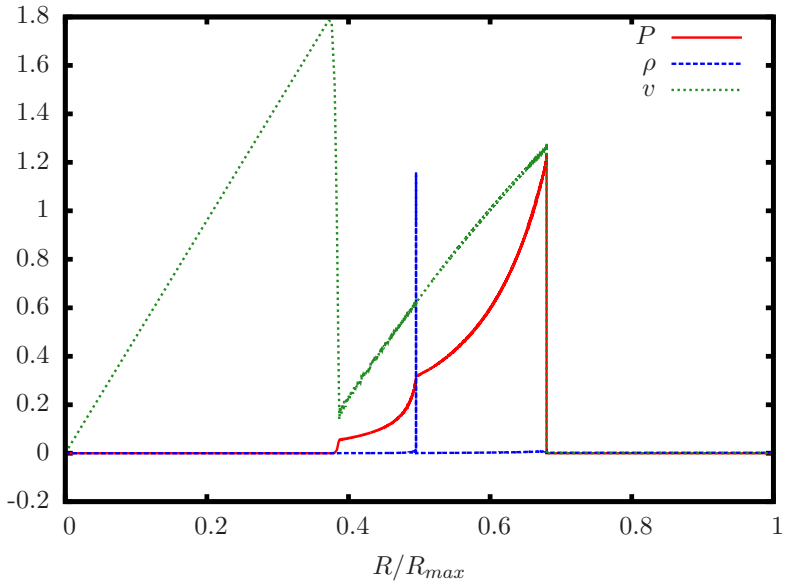

Figure 7.3: Pressure, density and velocity at t = 1027.28 yr and t = 2012.32 yr

7.4 Gaussian shell

Next we consider a similar distribution, a constant distribution with an addition: A shell at $r = 0.6$ pc, the shell has the from of a gauss curve. The shock trajectory was compared to the analytically solution for the constant density case and found to agree well, until the shock front hits the shell and the front slows down. The table below lists initial conditions. Note that r' is in units of 3.08×10^{18} cm and r'' in units for parsec.

M_s	E_s	R_s	T_a
$5M_\odot$	1×10^{42} erg	0.144 pc	10K
9.95×10^{33} g	1×10^{52} erg	4.44×10^{17} cm	10K
$\rho_a(r')$	Grid size	t_0	M_a
$1.67 \times 10^{-21}(1 + 50e^{-\frac{(r''-6)^2}{10^{31.5}}})\mathrm{kg/m^3}$	10pc	1yr	$214.5\mathrm{M}_\odot$
$1.67 \times 10^{-24}(1 + 50e^{-\frac{(r'-6)^2}{3.01\times10^{-5}}})\mathrm{g/cm^3}$	3.085×10^{19}cm	31 556 926 s	4.26×10^{35}g

Figure 7.5 and 7.6 shows the pressure, density and radial velocity at different times. $(P,\ \rho,\ v)$ The scales are given for velocity, density and pressure are given by:

$$v_s = 1.26 \times 10^5 \text{ m/s} = 1.26 \times 10^7 \text{ cm/s}$$
$$\rho_s = 8.35 \times 10^{-19} \text{ kg/m}^3 = 8.35 \times 10^{-22} \text{ g/cm}^3$$
$$P_s = 26.40 \text{ Pa} = 264.0\text{Ba}$$

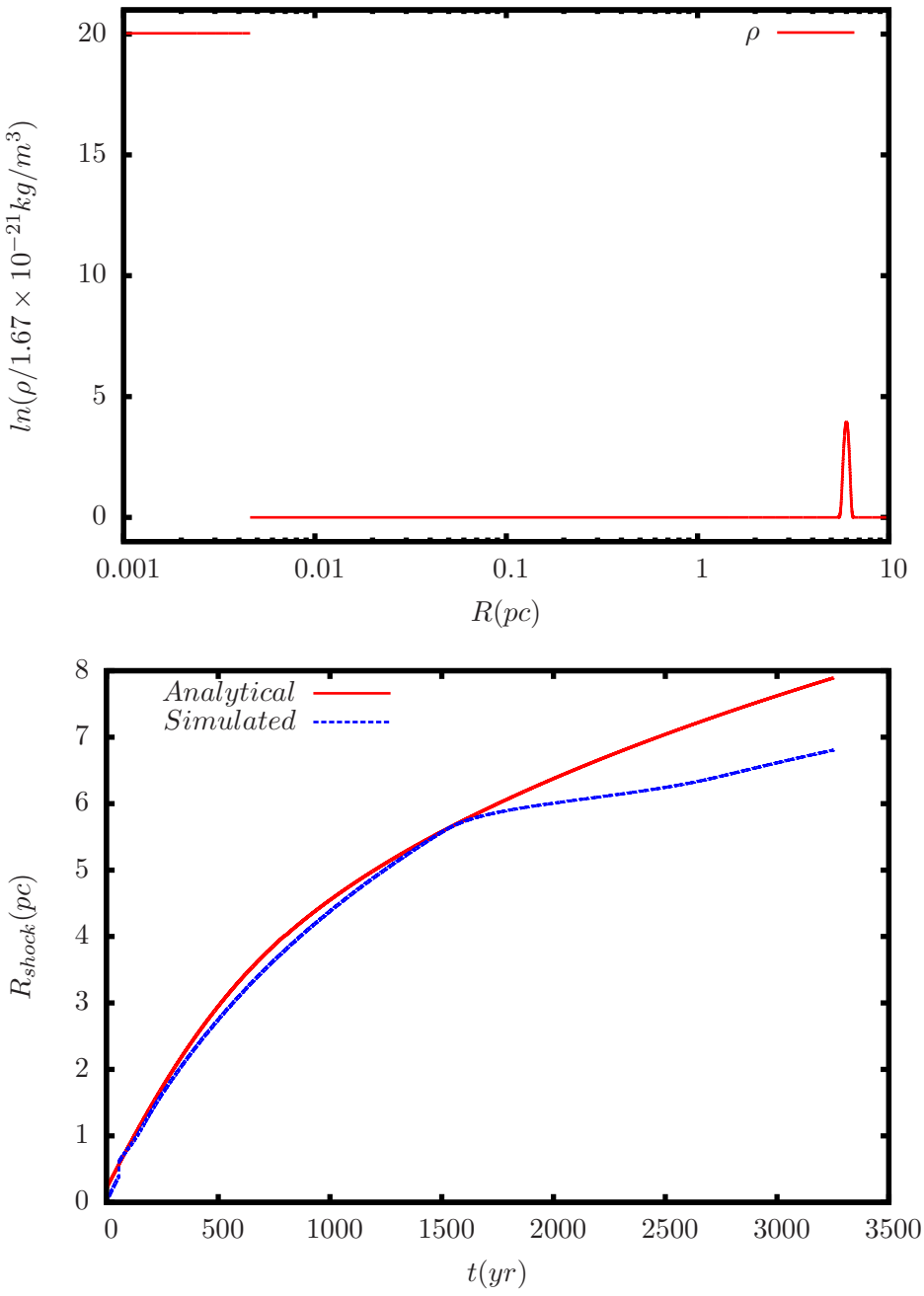

Figure 7.4: Density distribution and Shock trajectory

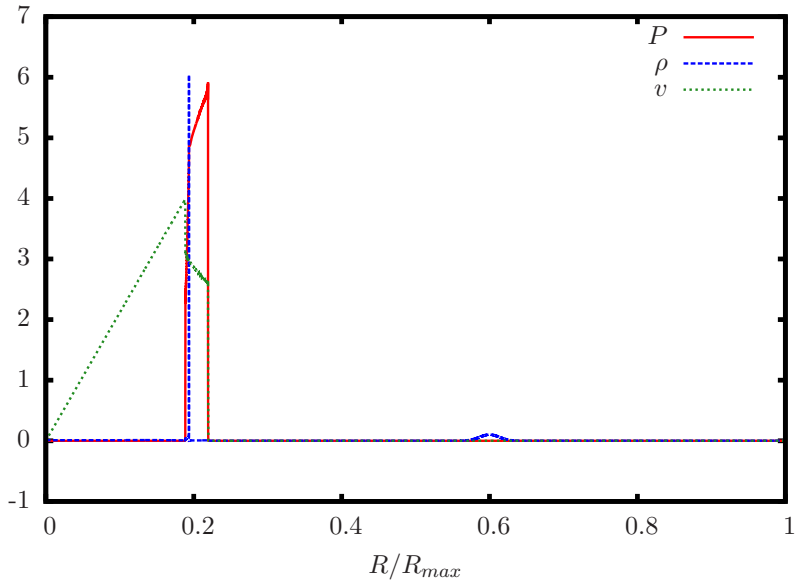

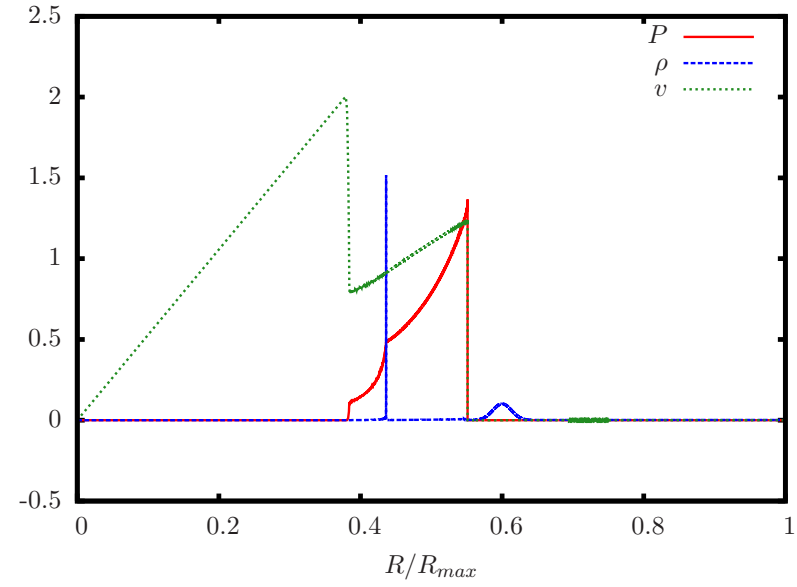

(a)

Figure 7.5: Pressure, density and velocity at t = 368.01 yr and t = 1473.02 yr

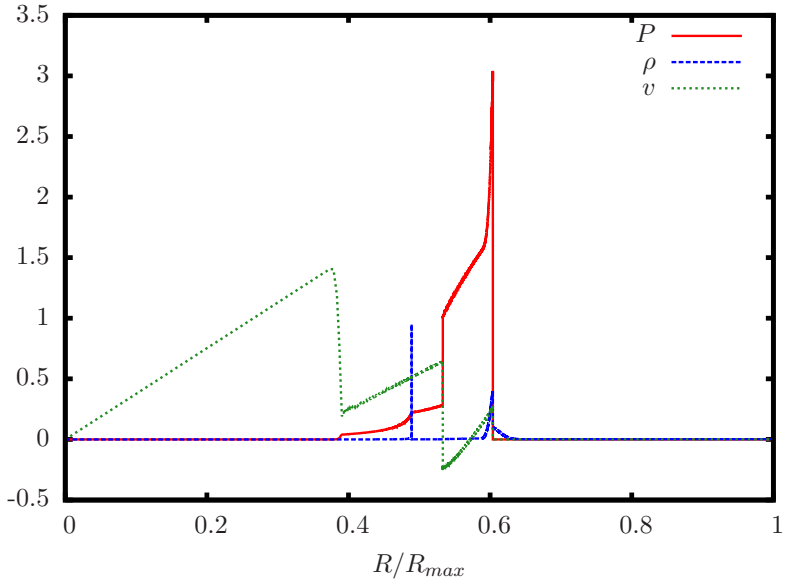

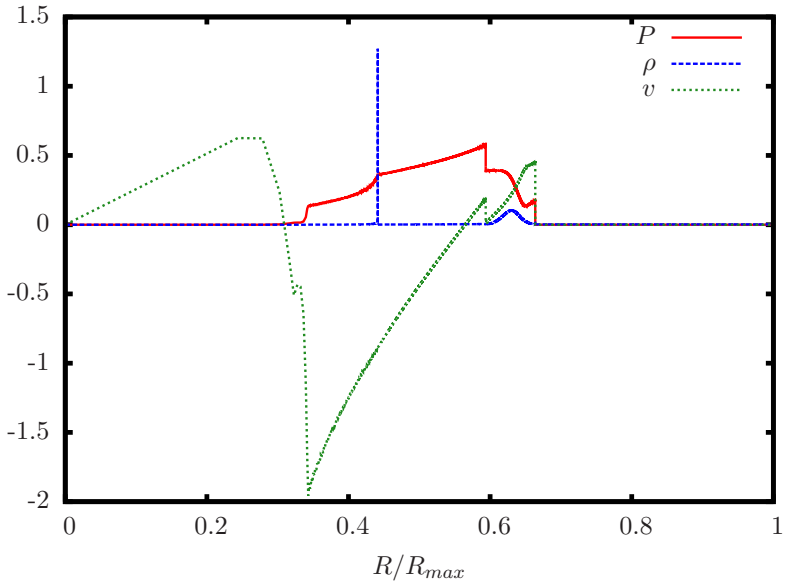

Figure 7.6: Pressure, density and velocity at t = 2067.37 yr and t = 3030.01 yr

7.5 Stellar wind

Stellar winds can create density profiles on the form $\rho \propto \frac{1}{r^2}$, see [14]. In this case it is possible to compare with analytical solutions.

M_s	E_s	R_s	T_a
$5M_\odot$	1×10^{44} J	0.144 pc	10K
9.95×10^{33} g	1×10^{52} erg	4.44×10^{17} cm	10K
$\rho_a(r)$	Grid size	t_0	M_a
$3.34 \times 10^{-18} r^{-2} \mathrm{kg/m^3}$	10 pc	1 yr	$0.13\mathrm{M}_\odot$
$3.34 \times 10^{-21} r^{-2} \mathrm{g/cm^3}$	3.085×10^{19} cm pc	31 556 926 s	2.58×10^{32}g

Figure 7.8 and 7.9 shows the pressure, density and radial velocity at different times. $(P,\ \rho,\ v)$ The scales are given for velocity, density and pressure are given by:

$$v_s = 8.80 \times 10^8 \text{ cm/s}$$
$$\rho_s = 8.35 \times 10^{-21} \text{ kg/m}^3 = 8.35 \times 10^{-24} \text{ g/cm}^3$$
$$P_s = 0.43 \text{ Pa} = 4.3\text{Ba}$$

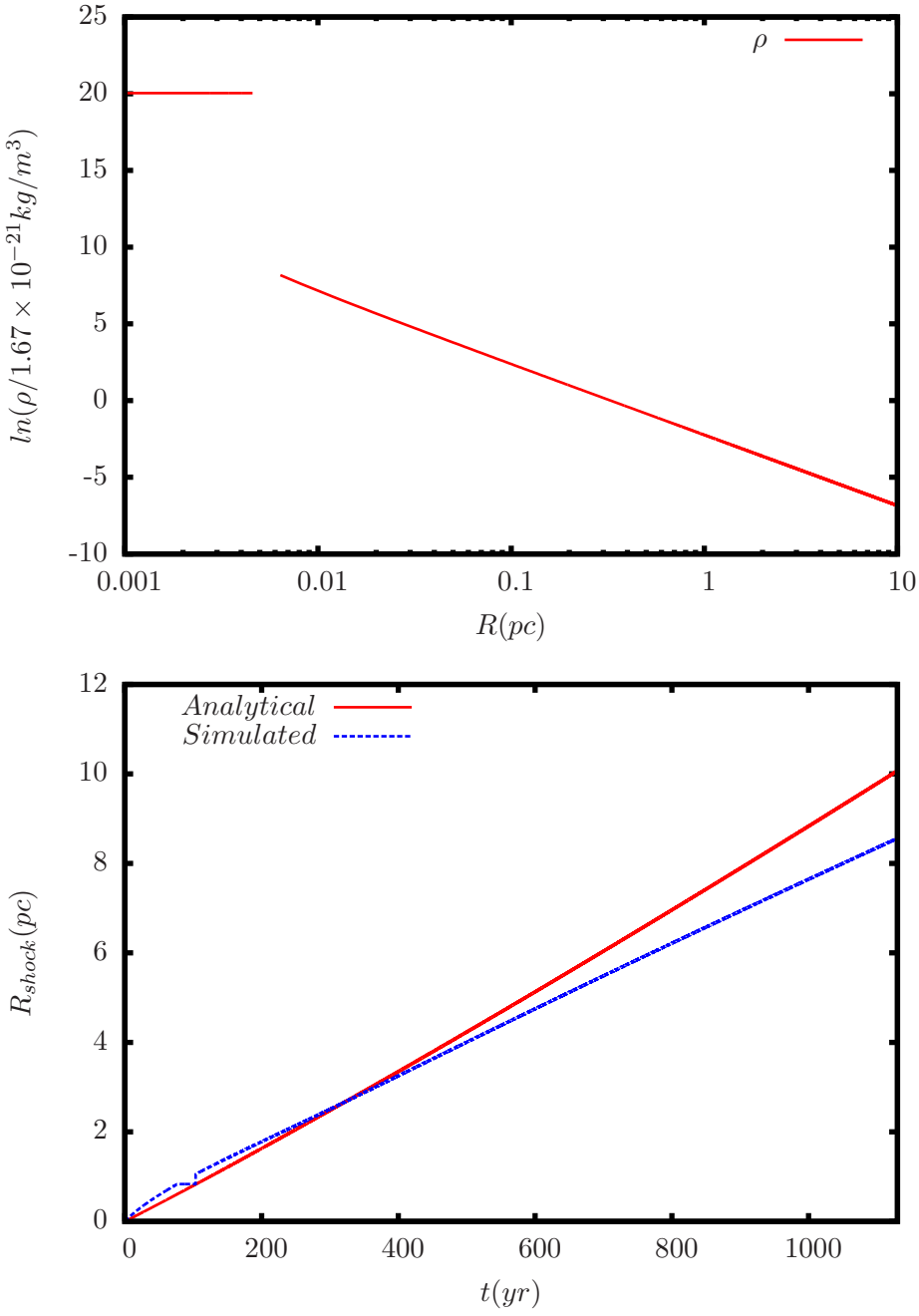

Figure 7.7: Density distribution and Shock trajectory

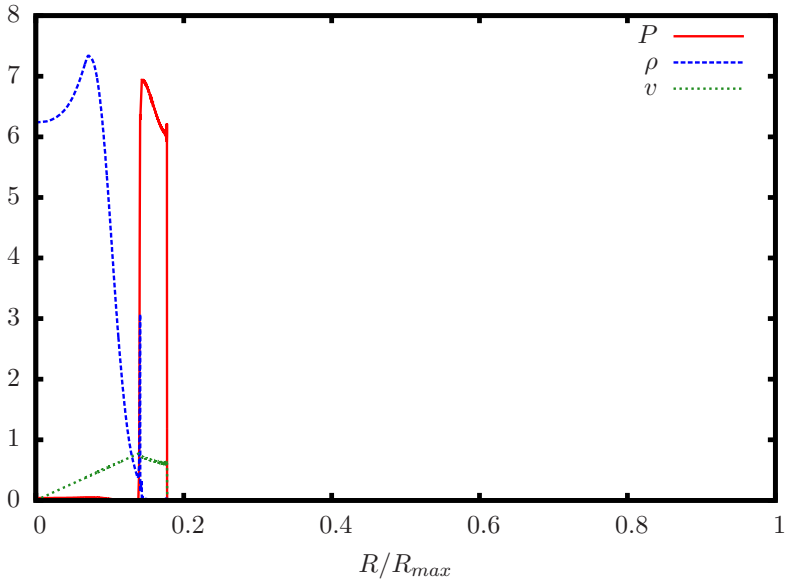

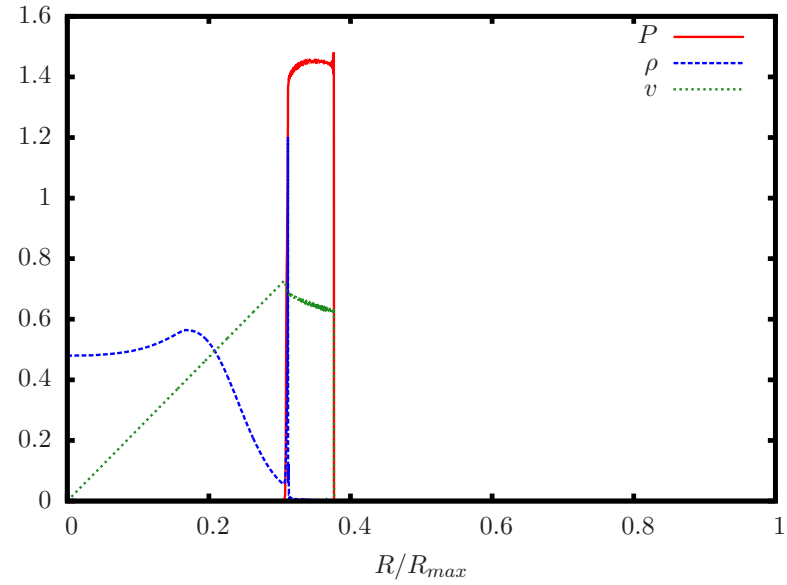

(a)

Figure 7.8: Pressure, density and velocity at t = 199.77 yr and t = 469.39 yr

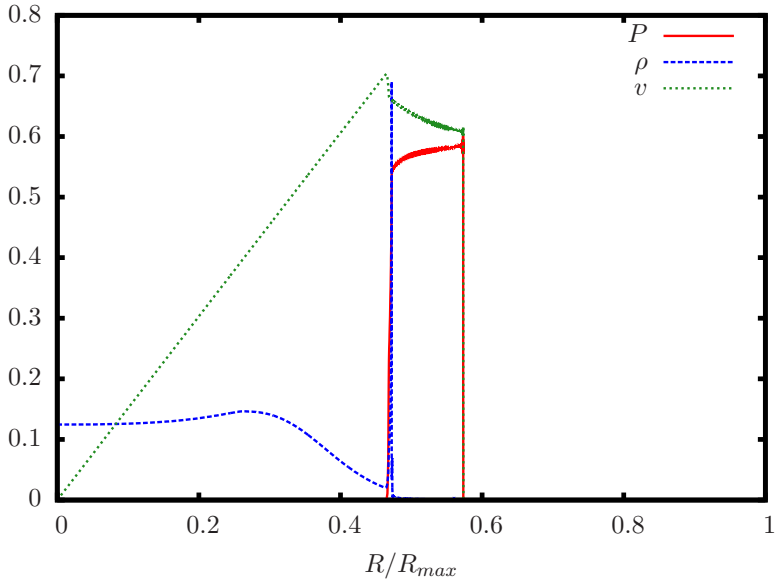

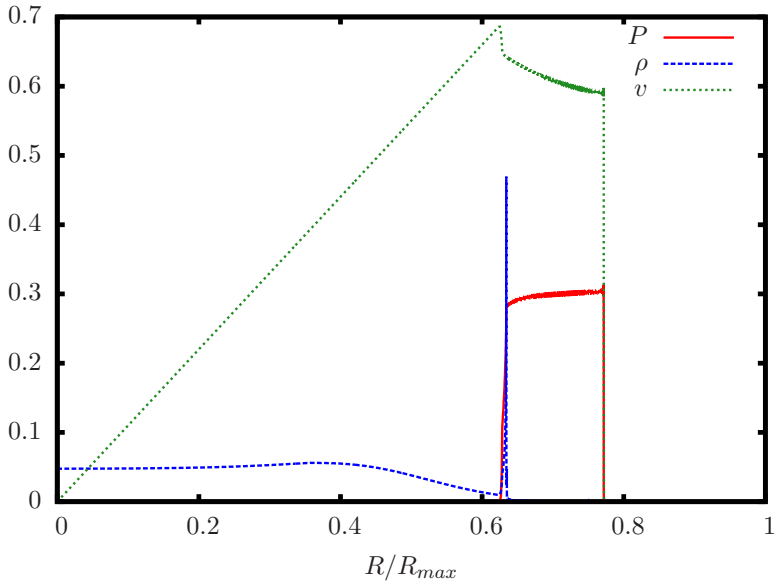

Figure 7.9: Pressure, density and velocity at t = 735.84 yr and t = 1013.26 yr

Chapter 8

Conclusions and outlook

In this thesis a supernova remnant is described by a set of hydrodynamic equations and those equations are solved numerically. The first order finite difference scheme produces results that agree well with analytic solutions, in the case of a constant ambient medium and a power law medium. For the cases where no analytic solution exists the code gives reasonable results, as expected the simulations produce a strong shock propagating forward trough the medium and a reverse shock moving backwards.

In the case of a gaussian shell we see that the shock trajectories follows the analytic solution, for a constant density profile. We see that the shock slows down, when it hits the shell. This is as expected.

When comparing the analytic shock trajectories with numerical simulations we see some deviation. The solutions put forward by Truelove and McKee is in the limit where $T \to 0$, however in the simulations a nonzero temperature has been used.

A natural next step would be to include a mechanism for radiation, this would make it possible to simulate the late stage evolution of the remnant. It could also be interesting to compare the simulations to observed events, this however would require some tuning of the initial conditions. Furthermore it would be interesting to look at cases without spherical symmetry, this would turn the problem into a multidimensional one and would require more computing power. As such it would have been beneficial to write parallel code, this could also be done in the one dimensional case to reduce the run time.

The results exhibit some unwanted behavior, the shock trajectory makes a jump in the start and the curves describing the pressure, density and velocity are not completely smooth everywhere. Since the discretization is only first order it would be an idea to implement an higher order method and see if this improves the result. On the other hand the necessity of this might be debated, the mentioned problems are small and the large scale behavior of the results are reasonable.

Appendices

Appendix A

Thermodynamics

Below we derive various thermodynamic properties of an ideal gas. Some knowledge about classical mechanics and quantum mechanics is assumed.

A.1 Microcanonical ensemble

Consider a classical system with Hamiltonian $H(p, q, t)$. For a given energy, E, there is a number of values for p and q satisfying $H(p, q, t) = E$. Each value of p and q corresponds to a microstate and a system with a given energy is called a macrostate. Note that many microstates can corresponds to the same macrostate, they defined a hyper surface in phase space given by:

$$S_E = \{\{p, q\} \mid H(p, q, t) = E\}\,. \tag{A.1}$$

The probability for a configuration of q and p where$H(p, q, t) = E$ is constant and if $H(p, q, t) \neq E$ the probability is zero. Assuming that each of the microstates, for a given energy, is equally likely to occur. As such the probability distribution is given by

$$P(q, p, t) = c\delta(E - H(p, q, t)), \tag{A.2}$$

here c is some normalization constant.

A microcanonical ensemble is the collection of all such microstates of a system with the same energy.

Entropy of a microcanonical ensemble is found by way of Bolzmanns equation,

$$S = k_b \ln W, \tag{A.3}$$

where W is the number of microstates with a given energy. For a microcanonical ensemble W is given by

$$W = \int \theta(E - H(p, q, t))dpdq, \tag{A.4}$$

here $\theta(x)$ denotes the Heaviside function.

From the first law of thermodynamics,

$$dE = TdS - PdV = \left(\frac{\partial E}{\partial S}\right)_V dS + \left(\frac{\partial E}{\partial V}\right)_S dV, \tag{A.5}$$

we see that

$$T^{-1} = \left(\frac{\partial S}{\partial E}\right)_V. \tag{A.6}$$

A.2 Ideal gas

Consider a volume, V, containing a gas of N non-interacting and identical particles. The Hamiltonian is given by:

$$H = \sum_{i=1}^{N} \frac{p_i^2}{2m}, \tag{A.7}$$

where p_i is the momentum of particle i and m is the mass of a single particle. Inserting equation (A.7) into equation (A.4) gives

$$W = \frac{1}{h^{3N}N!} \int_{E \geq H} d^3p_1..d^3p_N d^3q_1..d^3q_N, \tag{A.8}$$

where we have introduced the factor

$$\frac{1}{h^{3N}N!}.$$

This factor arises from quantum mechanics and can be understood from the uncertain principle,

$$\Delta q \Delta p \geq h, \tag{A.9}$$

and the fact that there is $N!$ ways to label N identical particles.

Since the Hamiltonian is independence of the spacial coordinates we can integrate them out and the momentum integral corresponds to a 3N-dimensional sphere with $r = \sqrt{2mE}$. As such W reduces to

$$W = \frac{2}{3N!N\Gamma(3N/2)} \left[\left(\frac{2m\pi E}{h^2}\right)^{3/2} V\right]^N. \tag{A.10}$$

Equation (A.3) together with equation (A.10) gives

$$
\begin{aligned}
S &= k_B \ln \left(\frac{2}{3N!N\Gamma(3N/2)} \left[\left(\frac{2m\pi E}{h^2} \right)^{3/2} V \right]^N \right) \\
&= k_B \left[-\ln\left(3N!N\Gamma(3N/2)\right) + \ln\left(2 \left[\left(\frac{2m\pi E}{h^2} \right)^{3/2} V \right]^N \right) \right] \\
&= k_B \left[N \ln V + \frac{3N}{2} \ln(\frac{4m\pi E}{h^2}) - \ln(3N) - \ln(\Gamma(3N/2)) - \ln N! \right] \\
&\approx K_B \left[N \ln V + \frac{3N}{2} \ln(\frac{2m\pi E}{h^2}) + \ln 2 - \ln(3N) - \right. \qquad \text{(A.11)} \\
&\left. \frac{3N}{2} \ln(3N/2) + \frac{3N}{2} - N \ln N + N + \ln N \right]. \qquad \text{(A.12)}
\end{aligned}
$$

In the last line we have used Stirling's approximation, $\ln N! \approx N \ln N - N$ for large N. This error we make is very small as long as N is large.

Gathering terms the last line in equation (A.11) simplifies to:

$$
\begin{aligned}
S &\approx k_B N \left[\ln \left(\frac{V}{N} \left(\frac{4\pi m E}{3Nh^2} \right)^{3/2} \right) + \frac{5}{2} + \frac{\ln(3/2)}{N} \right] \\
&= k_B N \left[\ln \left(\frac{V}{N} \left(\frac{4\pi m E}{3Nh^2} \right)^{3/2} \right) + \frac{5}{2} \right], \qquad \text{(A.13)}
\end{aligned}
$$

where in the last line $\frac{\ln(3/2)}{N}$ has been neglected, it is small for large N.

Taking the derivative with respect to E yields:

$$
\begin{aligned}
\left(\frac{\partial S}{\partial E} \right)_V &= k_B N \left(\frac{V}{N} \left(\frac{4\pi m E}{3Nh^2} \right)^{3/2} \right)^{-1} \\
&\quad \times \left(\frac{V}{N} \left(\frac{4\pi m}{3Nh^2} \right)^{3/2} \right) \times \frac{3E^{1/2}}{2} \\
&= k_B N \frac{3}{2E} \qquad \text{(A.14)}
\end{aligned}
$$

Since

$$
T^{-1} = \left(\frac{\partial S}{\partial E} \right)_V,
$$

we get:

$$
E = \frac{3}{2} k_B N T. \qquad \text{(A.15)}
$$

From this equation we can derive the specific energy: If M is the total mass of the gas then $M = Nm$ and energy per mass, $\varepsilon = E/M$, equals

$$\varepsilon = \frac{3}{2}\frac{k_B}{m}T. \tag{A.16}$$

If the energy is constant we know that $dE = 0$ as such

$$dE = TdS - PdV = 0 \Rightarrow \frac{P}{T} = \left(\frac{\partial S}{\partial V}\right)_E. \tag{A.17}$$

Equation (A.13) gives

$$\frac{P}{T} = \frac{Nk_B}{V}. \tag{A.18}$$

This is the equation of state for an ideal gas.

Bibliography

[1] M.R. Bate, I.A. Bonnell, and V. Bromm. The formation of a star cluster: predicting the properties of stars and brown dwarfs. *arXiv:astro-ph/0212380*, 2002.

[2] W. Benz. An introduction to computational methods in hydrodynamics. volume 373 of *Lecture Notes in Physics*, pages 259–313. Springer-Verlag, 1991.

[3] P. Bodenhimer, G.P. Laughlin, M. Rozyczka, and H.W. Yorke. *Numerical Methods in Astrophysics An Introduction*. Taylor and Francis, 2006.

[4] R.L. Bowers and J.R Wilson. *Numerical Modeling in Applied Physics and Astrophysics*. Jones and Bartlett Publishers, 1991.

[5] E. Cappellaro and M. Turatto. Supernova types and rates. *arXiv:astro-ph/0012455*, 2000.

[6] C.J. Clarke and R.F. Carswell. *Principles of Astrophysical Fluid Dynamics*. Cambridge University Press, 2007.

[7] ESA. The hipparcos and tycho catalogues, 1997.

[8] H. T. Janka et al. Core-collapse supernovae: Reflections and directions. *arXiv:1211.1378 [astro-ph.SR]*, 2012.

[9] M Ackermann et al. Detection of the characteristic pion-decay signature in supernova remnants. *Science*, 339:807–811, 2013.

[10] W-M. Yao et al. Cosmic rays. *J. Phys. G: Nucl. Part. Phys. 33 1*, 2006.

[11] M.L Kutner. *Astronomy A Physical Perspective*. Cambridge University Press, 2003.

[12] M.S. Longair. *High Energy Astrophysics*. Cambridge University Press, 2011.

[13] Dina Prialnik. *Theory of Stellar Structure and Evolution*. Cambridge University Press, 2000.

[14] J.K. Truelove and C. McKee. Evolution of nonradiative supernova remnants. *ApJS*, 120, 1999.

[15] J. VonNeumann and R. D. Richtmyer. A method for the numerical calculation of hydrodynamic shocks. *J. Appl. Phys*, 1950.

[16] B. Wang and Z.Han. Progenitors of type ia supernovae. *arXiv:1204.1155*, 2012.